Unveiling the sources of the catastrophic 1456 multiple earthquake: Hints to an unexplored tectonic mechanism in southern Italy

Umberto Fracassi and Gianluca Valensise

Abstract

We revisited data related to the 1456 seismic crisis, the largest earthquake to have ever occurred in peninsular Italy, in search of its causative source(s). Data about this earthquake consist solely of historical reports and their intensity assessment.

Due to the age of this multiple earthquake, the scarcity and sparseness of the data, and the unusually large damage area, no previous studies have attempted to attribute the 1456 events to specific faults. Existing analytical methods to identify a likely source from intensity data also proved inappropriate for such a sparse dataset, since historical evidence suggests that the cumulative damage pattern contains at least three widely separated events.

We subdivided the 1456 damage pattern into three independent mesoseismal areas; each of these falls onto E-W tectonic trends previously identified and marked by deep (>10 km) right-lateral slip earthquakes. Based on this evidence we propose (1) that the 1456 events were generated by individual segments of regional E-W structures and are evidence of a seismogenic style that involves oblique dextral reactivation of E-W lower crustal faults; (2) that each event may have triggered subsequent but relatively distant events in a cascade fashion, as suggested by historical accounts; hence (3) that the 1456 sequence reveals a fundamental but unexplored mechanism of tectonic deformation and seismic release in southern Italy. This style dominates the region that lies between the NW-SE system of large extensional faults straddling the crest of the southern Apennines and the buried outer front of the chain.

Although the quality of the available information concerning the 1456 earthquake is naturally limited, we show that the overlap of the damage distribution, the orientation and characteristics of regional tectonic structures, the seismicity patterns and the focal mechanisms all concur with our interpretations and would be difficult to justify otherwise.

Keywords: historical seismicity, macroseismic data, seismogenic faults, southern Italy

Introduction

The fold-and-thrust belt of the Apennines runs the full length of peninsular Italy and is the site of the largest number of Italian earthquakes. Although faulting mechanisms for most events are dominated by chain-perpendicular extension (among others: Meletti et al., 2000; Di Bucci et al., 2002; Montone et al., 2004; Valensise et al., 2004), the relationships between present-day faulting and the Apennines' tectonic fabric are highly diverse, subtle and potentially ambiguous (Valensise and Pantosti, 2001a). Depending on the area, large active structures (i.e., capable of producing earthquakes with $M > 6.5$) either (a) appear as newly formed faults not expressed at surface or not visible in seismic reflection profiles (Pantosti and Valensise, 1990), or (b) result from the coalescence of smaller faults (Di Bucci et al., 2002) and basins inherited from the original mountain building phases (e.g. Maschio et al., 2005).

Owing to its high population density and seismic risk, Italy's seismic safety depends on our ability to detect all potential seismogenic sources, starting with those that have already caused destructive historical earthquakes. Italian historical databases (Boschi et al., 1995, 1997; Monachesi and Stucchi, 1997; Boschi et al., 2000) and the parametric catalogs derived from them (Gruppo di Lavoro CPTI, 2004) are likely complete for the past 6-7 centuries and contain scattered evidence of

large earthquakes going back more than 2,000 years. Paleoseismic investigations of the causative sources of a few large destructive earthquakes suggest that recurrence times of individual large faults are comparatively long, consistently over 1,000 years and, in some cases, 3,000-5,000 years (Pantosti et al., 1993; Valensise and Pantosti, 2001b).

A total of 45 historical and instrumental earthquakes strong enough to produce severe damage and surface effects (M > 5.5; see Table 1) fall in our study area. Only 17 of these events have already been associated with a specific seismogenic fault using data from field mapping, landscape evolution, geophysics and paleoseismology (DISS Working Group, 2006, and references therein). Sources based on macroseismic (intensity distribution) data alone have been proposed for 15 of the remaining strong earthquakes (for a summary: Valensise and Pantosti, 2001b). Bearing in mind that historical earthquakes obviously lack a known focal mechanism, the reason that seismogenic sources were determined preferentially for the stronger earthquakes is a result of the fact that they caused higher and more widespread damage, more surface effects and more historical accounts, all of which helped in identifying their causative faults.

The damage area of the 1456 sequence is very large (~18,000 km^2), and ~ 6% of the entire Italian territory suffered intensity ≥ VIII effects on the Mercalli-Cancani-Sieberg scale; (Fig. 1; Magri and Molin, 1983; Meletti et al., 1988). Owing to its intensity distribution, its presumable magnitude and to the fact that its intensity field certainly contains effects from multiple shocks, thus prevcnting the identification of discrete events, the 1456 earthquake is the most important in this group of catastrophic events that still lack a plausible causative source. The area affected by the 1456 sequence extends from central Italy (to the north) to Apulia (in southeastern Italy) and from the Adriatic to the Tyrrhenian coasts (Fig. 2). The maps in Fig. 1 show three or more distinct high intensity *mesoseismal areas* (areas bearing peak damage) separated by "intensity troughs" (that is to say, areas characterized by lower intensities, not by lack of data). The (a) extent of the entire damage area, (b) the existence of

three separate areas of concentrated damage in three different, widely separated seismotectonic contexts, and (c) the diverse structures and terrains therein, all suggest that multiple sources must have created the damage pattern, and that such prospective sources are rather distant from one another. This implies that the 1456 earthquake is in fact made of multiple destructive events. Finally, because of the tectonic fabric of central and southern Italy and the style of active deformation documented by earthquake data (for a summary see Valensise et al., 2004), the causative faults of the 1456 events are likely to be quite different from the normal faults thought to be responsible for the main destructive earthquakes of the southern Apennines.

Besides proposing that several independent sources have caused the 1456 events, we also demonstrate that this earthquake sequence offers new insight into several events that have occurred east of the southern Apennines axis, particularly within the Apulian foreland (Fig. 2). The Apulian domain was commonly considered a rather aseismic region in Italy (Meletti et al., 2000; Del Gaudio et al., 2005). This explains why the relatively small 31 October-1 November 2002, M_w 5.8 Molise earthquakes (Di Bucci and Mazzoli, 2003; Pondrelli et al., 2003; Valensise et al., 2004; Vallée and Di Luccio, 2005; Chiarabba et al., 2005) had a major impact on the Italian seismic hazard scenario and forced the seismological community to reconsider the role of such "minor events" at the scale of the entire southern Apennines (see: Gruppo di Lavoro MPS, 2004). Because most of these smaller earthquakes overlap areas of high 1456 intensity, their occurrence and macroseismic pattern emphasize the importance of subtle yet key features of the 1456 damage scenario.

The ideas and interpretations presented in this paper are based on an extensive and complex dataset of historical, instrumental and tectonic data. To streamline our reasoning, this work is organized as follows:

1) overview of the regional seismotectonic framework;

2) analysis and discussion of available historical references for the 1456 sequence;

3) break-down of damage into areas of maximum damage;

4) definition of relative and absolute timing for the inferred events;

5) preliminary identification of macroseismic sources based on intensity data alone;

6) final identification of seismogenic sources for the primary shocks based on all available data.

Geological and seismotectonic features of the Southern Apennines

Main features of Central and Southern Apennines

The Apennines fold-and-thrust belt of peninsular Italy is one of the outcomes of the convergence between the African and European plates that started in the Late Cretaceous (Mazzoli and Helman, 1994). Gravity-induced sinking of the lithosphere beneath the Adriatic and Ionian Seas and related subduction rollback (Patacca and Scandone, 1989) are believed to have driven thrust accretion across the Adriatic continental margin and extension in the Tyrrhenian back-arc.

The Apennines developed because of the deformation of two major paleogeographic provinces: (a) an internal terrane that includes late Jurassic to Oligocene tectono-sedimentary sequences of the Ligurian-Piedmont Ocean, and (b) an external terrane, composed of Triassic to early Miocene sedimentary rocks derived from the deformation of the continental Adriatic-African passive margin (see Butler et al., 2004, for a review). Starting from Oligocene time, the tectonic units were transported towards Adria, resulting in several tens of km shortening of the Apennines (Patacca and Scandone, 1989, and references therein). Mainly E- to NE-directed thrusting and associated foredeep/ thrust-top basin sedimentation progressed toward the Adriatic foreland at least up to middle Pleistocene time.

Our study area includes the central and southern part of the Italian peninsula (Calabrian arc excluded), where the Southern Apennines orogenic stack and the Apulian foreland are composed of two carbonate platforms (the Apennine and Apulia platforms) separated by the Molise-Sannio-Lagonegro pelagic basin (Butler et al., 2004, and references therein; Fig. 2). Oil-industry wells that were drilled through the tectonic units of the Apennine platform, the Molise-Sannio-Lagonegro basins and related foredeep deposits, have reached deep platform units that are the buried western continuation of the Apulian foreland (Mostardini and Merlini, 1986; Menardi-Noguera and Rea, 2000). Analyses of synorogenic deposits indicate that the allochthonous units of the Apennine platform and pelagic basin were accreted by thrust faulting mainly in Miocene times, while deeper thrusting involving the Apulian platform began in early Pliocene - early Pleistocene time (Butler et al., 2004, and references therein).

Several investigators (e.g. Hippolyte et al., 1994) have proposed that a major geodynamic change occurred around 800 ka BP, when the dominant tectonic regime of peninsular Italy became extensional. Chain-perpendicular extension still dominates throughout most of the Apennines, as shown by borehole breakout, seismicity and recent GPS data (Oldow et al., 2002; D'Agostino and Selvaggi, 2004; Montone et al., 2004; Serpelloni et al., 2005, 2006).

Seismotectonic overview: sources and kinematics

The mechanisms responsible for earthquakes in southern Italy have been thoroughly documented in the past 20 years, largely in the aftermath of the catastrophic 23 November 1980, M 6.9 Irpinia earthquake (Deschamps and King, 1984; Pantosti and Valensise, 1990; Amato and Selvaggi, 1993; Boschi et al., 1993; Giardini, 1993; Valensise and Pantosti, 2001a; Ascione et al., 2003; Improta et al., 2003). Most strong earthquakes in the Southern Apennines occur along a segmented belt of large normal faults running along the crest of the Apennines. This was identified early on as "*Faglia Sud-*

Appenninica" (i.e. "Southern Apennines Fault System"; Pantosti and Valensise, 1988) and later investigated by a number of workers (see Valensise and Pantosti, 2001a, b, and DISS Working Group, 2006, for a review). These large faults dip predominantly to the southwest in the Central Apennines and to the northeast in the Southern Apennines, excluding the Calabrian Arc (DISS Working Group, 2006).

Although ridge-top normal faulting accounts for much of the seismicity of peninsular Italy, several major earthquakes that took place in central and southern Italy are in contrast with this simple model (e.g. 1361, 1466, 1627, 1694, 1731, 1930, 1981; see Table 1 for corresponding IDs in Fig. 3). For instance, the 1694 and 1980 earthquakes (both M 6.9; ID # 21 and 68, respectively) exhibit damage areas of similar extents, orientation and region of maximum intensities, yet the 1694 event did not cause slip on the fault responsible for the 1980 earthquake (Pantosti et al., 1993; intensity data in: Boschi et al., 2000). Similarly, the source of the 26 July 1805, M 6.6 Boiano earthquake (ID # 30) sits in the core of the damage area of the 1456 sequence, but paleoseismological data (Blumetti et al., 2000; Galli and Galadini, 2003) indicate that its causative fault did not slip in 1456.

A few additional lines of evidence emphasize the complex nature of the regional tectonics. The 15 January 1466, M 6.1 Irpinia earthquake (ID # 14), that occurred in the Irpinia 1980 epicentral zone, exhibits a damage pattern totally different from that of the 1980 earthquake; this fact too suggests either a different source or a different faulting mechanism (or both) for two significant earthquakes that have virtually coinciding epicenters (data in: Guidoboni and Comastri, 2005). Furthermore, the ~2,000 years recurrence time estimated for large earthquakes like the Irpinia 1980 one (Pantosti et al., 1993) does not support the occurrence of two large events on the very same fault in a 500-year-long timespan. A larger earthquake (M 6.7) took place on 23 July 1930 (ID # 51) in the eastern sector of the same area, a particularly complex region dominated by the presence of the extinct Vulture volcano. Instrumental data and new analyses (Jiménez, 1991; Ferrari et al., 2002; Emolo et al., 2004) suggest

that this earthquake ruptured a nearly E-W plane with a dip-slip mechanism having a dextral component.

Finally, a number of smaller yet significant events (M < 6) that have unexpectedly greater focal depths of ~15-20 km and right-lateral strike-slip kinematics have occurred in the eastern portion of the study region in the past 35 years; they are the 6 May 1971, Monteleone (M 5.2; ID # 62), the 5 May 1990 (M 5.8; ID # 72) and 26 May 1991 (M 5.2; ID # 73), Potenza, the 16 July 1992, Guardiagrele (M 4.3; ID # 74), and the 30 October-1 November 2002, Molise earthquakes (both M 5.8; IDs # 76 and 77, respectively), plus a number of minor ones (Frepoli and Amato, 2000). All these earthquakes supplied instrumental evidence for the presence, activity and seismogenic potential of deep faults (> 10 km) roughly oriented E-W along the eastern sector of central and southern Italy between 40.5° and 42.5°N.

In short, a combination of historical and instrumental evidence indicates the existence of a previously unrecognized set of large earthquake sources in southern Italy. Such faults would be part of a system that is either independent from the above mentioned Apennines-top array, or that somehow interacts with it to the extent allowed by the present-day stress field. As stated earlier, both instrumental seismicity (Amato and Selvaggi, 1993; Milano et al. 1999, 2002; Castello et al., 2006) and geological data (DISS Working Group, 2006, and references therein) suggest that most major southern Apennines earthquakes occur in the uppermost 10-12 km of the crust in the core of the thrust-belt. This "shallower dip-slip vs. deeper strike-slip" scenario may well explain the complex 1456 sequence.

The 1456 earthquake sequence

Coeval historical references: importance and limits of the data

The 1456 seismic crisis consists of at least two well constrained and similarly large mainshocks, the first on 5 December and the second on 30 December (Magri and Molin, 1983; Meletti et al., 1988; Boschi et al., 2000; Guidoboni and Ferrari, 2004; Guidoboni and Comastri, 2005). The maximum damage was reported in historical references (i.e., letters, official statements, reports of property damage) dated from 5 to 10 December, and must hence be attributed to the first mainshock. Several relatively well documented aftershocks occurred throughout the rest of the month, until the second mainshock took place (Guidoboni and Comastri, 2005). The sequence continued up to early 1457, causing further damage. Less frequent aftershocks of decreasing intensity continued from March to the end of May 1457 (Boschi et al., 2000; Guidoboni and Comastri, 2005).

We thoroughly examined the historical accounts presented and discussed in previous studies. We also analyzed the earthquake intensities using an automatic algorithm (Gasperini et al., 1999). This technique employs empirical relationships and attenuation laws to compute the epicenter, moment magnitude (M_w), size and strike of a causative source based entirely on macroseismic data. However, the age of the events and the unknown nature of their causative sources made it difficult to associate each phase of the sequence with a specific area. Besides, the original earthquake accounts were written using a sophisticated phrasing that sometimes goes beyond the mere stylistic accuracy, Such an enriched language derives in part from the age of writing and in part from the fact that the reports were written by representatives of the centralized administrations of the XV century (Guidoboni and Comastri, 2005):

a) the Naples Kingdom ("Regno di Napoli" or "Regno delle Due Sicilie"), which included all territories struck by the sequence;

b) the Vatican State ("Stato della Chiesa");

c) the consulates of foreign powers (mainly Castilla and Catalunya, i.e. present-day Spain);

d) noble families of Milan ("Ducato di Milano") and Florence ("Signoria di Firenze").

The letters containing these accounts would need considerable time for traveling from the place of writing (bearing the effects of the earthquake) to the head administrations in Naples, Rome, etc. In addition, the accounts were sometimes tailored for the specific purpose of demonstrating that all possessions were destroyed – or denying it. Deceptive and secondary as this may seem, such constraints do apply to the socio-economic portrait of the Naples Kingdom during the XV century. As such, the semantics and style of the reports must be interpreted carefully when attempting to ascertain the dates and effects of the earthquakes.

The macroseismic dataset that we used for this study was based on *a)* the re-evaluation of the 1456 effects described by Guidoboni and Ferrari (2004) and *b)* our critical review of reports whose location and damage are uncertain and/or poorly documented. The former dataset was obtained from a partnership between INGV (Istituto Nazionale di Geofisica e Vulcanologia) and SGA (Storia Geofisica Ambiente, Bologna, Italy), a private consulting firm that specializes in historical research, to complete and improve the available information. The result was a thorough historiographic review that led to the discovery of new damaged sites (from previously unknown coeval sources), improvement of the damage assessment and intensity patterns, and an accurate cross-check of the demographic distribution of central and southern Italy in the XV century.

Main features and breakdown of the intensity pattern

The macroseismic dataset prior to the review of the available and new historical sources contained the sum of earthquake effects for the entire sequence. In this work, we show the revised intensity values, distinguished for the main individual shocks composing the sequence (Table 2), and the location and boundaries of the areas of maximum damage (Fig. 4). The intensity pattern exhibits various distinct features:

1) the distribution of data in the different intensity classes is very uneven; in particular, there is a general lack of lower intensities (below VIII). Although historical catalogs of strong earthquakes (see: Boschi et al., 2000) show that such a characteristic is not unusual for old large events (i.e., coeval sources tended to assess only major damage), it is strikingly evident for this case;
2) despite the severity of the 1456 earthquakes, the damaged sites are remarkably sparse compared to the intensity distribution of other large nearby earthquakes such as the 1805 Molise event (data from Boschi et al., 2000). A possible explanation can be the age of the sequence, which in many cases resulted in scarce and/or lost information. Based on the level of damage and the inferred ground shaking effects across the entire region, currently undiscovered historical accounts might still be missing to fill in the intensity record. In fact, not all localities known to have existed in 1456 are listed in the damage reports (Guidoboni and Comastri, 2005);
3) the sites that reported intensities above the damage threshold (≥ V-VI) cover a much broader region than the one caused by any other major earthquake of central and southern Italy. This is best shown by the V/V-VI intensity associated with L'Aquila (42.356° N, 13.396° E) and Lecce (40.351° N, 18.169° E; see Table 2), over 450 km apart. This long distance is very significant when compared with the 340 km distance between the farthest intensity V datapoints for the 23 November 1980, M 6.9 Irpinia earthquake (Paola, northern Calabria, and Pescara, central Italy; data in Boschi et al., 2000).
4) the spatial distribution of peak intensities is wide and seemingly trendless (Fracassi and Valensise, 2004). In contrast to other destructive historical events, X-XI damage occurred continuously across most of the study area over a distance of nearly 180 km, strongly suggesting that distinct sources, distant from one another, best explain such a large mesoseismal area.

Fig. 5 shows the three areas of peak damage, labeled *a*, *b* and *c*, from north to south). We remark that historical reports mentioning the cities of Roma and Recanati (in central Italy) and those of Cosenza, Crotone and Messina (in southwestern Italy) were written several years to tenths of years after 1456 and were thus deemed unreliable (Guidoboni and Ferrari, 2004). Moreover, because of their location and low intensities (III, IV), these localities were irrelevant to this study and are not listed here. The areas shown in Fig. 5 are named after the main localities that reported the highest intensities.

a) Caramanico – Tocco Casauria

This region is characterized by the intensity X-XI reported at Caramanico, which is located on the western shoulder of the Maiella Mt. The IX-X value at Tocco Casauria and the IX at Castiglione Casauria and Torre de' Passeri surround this site. From Sulmona (to the southeast) towards Navelli and the lower Aterno Valley (to the northwest), intensities range between VIII and IX. While these high intensities span a ~40 km-wide area in a southeast to northwest direction, the intensity drops to V within a distance of ~20 km to the west (L'Aquila) and to the east (Chieti).

b) Isernia-Boiano

This area contains two intensity XI datapoints (Boiano and Isernia) and several intensity X datapoints extending from Acquaviva d'Isernia (northwest) to Santo Stefano (northeast) to Cercemaggiore (southeast). The intensity IX datapoints cover a very broad area ca. 75 km across, from Isernia to upper Sannio. In particular, high intensity areas are: a) from Isernia to the upper Sangro River valley (Pescocostanzo, VIII); b) Castellino del Biferno – Campobasso, towards Santo Stefano; and c) northeast of the Matese massif, with X and XI sites like Boiano. A few high intensity datapoints fall northeast of these groups (Sprondasino and Castelluccio Acquaborrana, IX).

c) Ariano Irpino-Paduli

This portion of the mesoseismal area displays intensity XI sites at Ariano Irpino, Apice, Paduli and Pesco Sannita (from east to west). Various intensity X datapoints lie within this region, from Limata (west) to San Marco dei Cavoti (northeast) and Mirabella Eclano (southeast). Intensity IX datapoints also occur towards the southwest (e.g. Roccarainola), while a number of intensity VIII are present to the northeast (e.g. Troia).

Chronological and spatial sequence of damage

The recent historiographic review of the 1456 sequence attempted to subdivide the earthquake effects into possible time windows using a) descriptive linguistic parameters in contemporary reports and b) a comparison between reported victims for a given locality and the actual number of inhabitants prior to the events (Guidoboni and Ferrari, 2004). An example for point a) is the locality of Apice, described with dramatic Latin adjectives (*"eversum radicitus"*, that is "overthrown at the roots"), sometimes repeated and redundant throughout a report. An example for point b) is the case of Isernia, that suffered catastrophic damage (intensity XI) and large human loss (1,500 victims out of 2,035 inhabitants; comparison made with previous census).

After a cross-check and a critical review of the damage information from numerous revised sources, we propose a scenario that involves a sequence of shocks (Fig. 6). Severe damage was first reported in the southern portion of the region, and then progressively towards the north during the seismic sequence. The first shock occurred on 5 December and several accounts reported major damage in Sannio at Apice, Ariano Irpino, Casalduni and Paduli, and at some localities in the Capitanata (Fig. 6a). According to several historical references, primary damage occurred in Napoli and in the entire Piana Campana.

Two possible aftershocks occurred on 11-12 and 21-22 December. Historical accounts for the 11-12 December (Fig. 6b) reported destruction in the Sannio (Apice, Ariano Irpino and Paduli), and 70 km to the north of Apice, in Isernia (to the west), Campobasso and in the Capitanata (to the east) and Murge areas; Castel di Sangro, 30 km north of Isernia, also experienced major effects. Historical sources for 21-22 December (Fig. 6c) reported cumulative damage for the whole sector between the Sannio and Matese areas from Paduli to Limata and Isernia (from south to north), including the western Capitanata. We believe that reports for the night between 21 and 22 December hint at a real earthquake that occurred in areas already severely struck by the earlier mainshock (Guidoboni and Ferrari, 2004). On the other hand, constraints for the night between 11 and 12 December are less certain and we can thus only tentatively associate such reports with a real aftershock.

A second major earthquake occurred on 30 December, although reviewed descriptions (Guidoboni and Ferrari, 2004) indicate that damage reported in Sannio and Piana Campana may include the cumulative effects of the previous event(s) (Fig. 6d). In Napoli, this event was perceived as less destructive than the 5 December shock (Magri and Molin, 1983; Meletti et al., 1988; Guidoboni and Ferrari, 2004; Guidoboni and Comastri, 2005). Heavy damage was reported in Isernia, east of the Matese and in the Sannio region. Beginning with the earthquake of 30 December, sites in Abruzzo (chiefly Tocco Casauria) reported major effects; other adjacent localities can be associated with the same time window. Based on data by Viti (1972) and Cozzetto (1986), Guidoboni and Comastri (2005) show that localities between Sulmona and Castel di Sangro are separated by a group of localities that did not report damage.

In mid-January 1457 (on the 8th or 9th of the month, according to Guidoboni and Ferrari, 2004), a new shock severely damaged the Sannio and Matese regions (Fig. 6e), with reports describing effects from Ariano Irpino in the south and Tocco Caudio to Isernia and Frosolone to the north, including Napoli. Reports for the later part of the sequence describe damage in the entire region east of Isernia.

Finally, a comprehensive account, written in 1457 by Giannozzo Manetti, a scholar of the Florence court, describes in detail the effects for 153 localities (Guidoboni and Ferrari, 2004), but does not supply any information on when damage occurred. However, this source is remarkably reliable from an historical viewpoint and contains unique linguistic descriptions and a homogeneous and self-consistent portrayal of intensities (Guidoboni and Comastri, 2005). The account by Giannozzo Manetti describes several localities not known to other contemporary local sources and therefore not yet associated with an event of the sequence. We separated such datapoints from the main list (Fig. 6f) and noticed that almost all such sites fall on the Adriatic coast (i.e. from Penne to Lecce) and between the regions of Irpinia and Murge (Melfi). Other localities fall west of the Capitanata (Volturino) and in the inner Sannio (Frigento) regions. Based on the intensity distribution and the relationships with other mesoseismal areas, we interpret the region of lower damage (V-VI) on the Adriatic coast as far-field effects of the mainshocks of 5 and 30 December and the area of higher intensities (VIII and IX) between the Murge and Irpinia regions as part of the damage caused by the 5 December event.

A final note concerns the date of written reports. By plotting the sites mentioned by each historical reference and considering the known dates of the mainshocks (5 and 30 December), we deduce that most reports were written from one to several days after the given earthquake whose effects were described. Because of this, we group data from one or more historical references when the effects mentioned can be attributed to the known mainshocks. These associations directly affect our magnitude estimates for the inferred events.

In synthesis:

i) on 5 December, the earliest mainshock occurred in the Sannio region (Fig 5c) and heavily affected Napoli and the surrounding area;

ii) a mid-December aftershock occurred in the Ariano Irpino-Paduli region (Fig 5c) and another event occurred in the Isernia-Campobasso area (Fig. 5b);

iii) on 21 December a large aftershock hit the Ariano Irpino-Paduli area (Fig. 5c);

iv) the 30 December mainshock occurred in the Caramanico area (Fig. 5a), while in the same day another earthquake took place in the Isernia-Campobasso area (Fig. 5b);

v) further aftershocks occurred on 8 January 1457 in the Isernia-Campobasso (Fig. 5b) and Sannio (Fig. 5c) areas.

Seismogenesis of the 1456 main events from historical evidence

Peculiarities of the 1456 macroseismic pattern

As previously discussed, damage reported for the 1456 earthquake is distributed in widely separated areas. In addition, the intensity pattern shows extensive and elongated strong-damage areas, unlike the prevailing damage distribution caused by destructive earthquakes in the southern Apennines shown by the data supplied by Boschi et al. (2000). These observations raise two fundamental questions: 1) where are the sources? and 2) what are their geometry and kinematics?

Concerning the location of the sources, the separate and distant epicentral areas defined by the historical damage reports provide strong evidence for distinct individual sources. Since these sources are not adjacent to one another, their parameterization using automatic treatment of intensity data is not straightforward (Fig. 7). Regarding the source geometry and kinematics, numerous studies show that the majority of destructive events (M_w > 6.5) along the Apennines belt were caused by pure normal faulting sources, including the 26 July 1805, Molise (M_w 6.6) and the 23 November 1980

Irpinia (M_w 6.9) earthquakes (for a summary: Valensise and Pantosti, 2001b; DISS Working Group, 2006 and references therein).

We infer that the location, geometry and kinematics of the causative faults of the 1456 main events have little in common with the sources of the above mentioned earthquakes. On the whole, these peculiarities strongly suggest that the 1456 sequence was generated in a tectonic context unknown to most studies on the seismotectonics of southern Italy.

Source hypotheses from intensity data (macroseismic sources)

Based on the spatial-temporal distribution of damage from historical accounts, we attempt to define individual seismogenic sources, hereafter *macroseismic sources*, using the Boxer code (Gasperini et al., 1999) and the intensity data of Table 2. To briefly explain the functions of this code, Boxer computes (a) the earthquake epicenter and (b) its moment magnitude from intensity data. Concerning (a), the code groups intensity classes and calculates corresponding isoseismal radii; to minimize biased intensities resulting from site amplifications and other sources, the system employs the median isoseismal value as a central tendency estimator. With respect to (b), the code computes the distance between the epicenter and each available locality, using the median as central tendency estimator. Boxer then follows a statistical approach, using a bivariated weighted regression to fit each intensity class and associate it with a magnitude value. A weighted magnitude is then computed

We propose the following three discrete *macroseismic sources*, numbered ***1*** to ***3*** in their order of occurrence and named after the areas they affected (Fig. 7). Recall that these sources result from the automatic treatment of intensity data and therefore derive from calculations, not from geological evidence. The physical constraints that allow us to build a geologically plausible source based on the information provided here will be introduced in the following chapter.

*Source #**1** (Piana Campana – Irpinia – Sannio – Murge – Salento)*

Historical accounts show that damage in this large region occurred during the early stages of the sequence. We attribute it to the 5 December mainshock and to the 11-12 and 21-22 December aftershocks, which also caused severe damage and accumulated earthquake effects. Three observations indicate that this was a large earthquake generated by a deep (> 10 km) source:

a) Sites reporting maximum intensities are widely spaced, with minimal intensity decay moving farther from the epicentral area;
b) The widely distributed X and XI intensities show trends oriented NW-SE and E-W. While the former orientation may be due to the concentration of localities within the Apennine landscape (a system of NW-SE trending mountain fronts and intermontane basins), the latter has no obvious explanation;
c) The damage belts contain consistently high intensities throughout (Fig. 5c).

*Source #**2** (Matese – Gargano)*

This region was affected by the mid- and late-December events. Consistently high intensities (X and XI) occurred (a) in Isernia and nearby, (b) along a NW-SE trend from Macchiagodena toward Castelluccio Acquaborrana, and (c) along an E-W trend from Boiano to Cercemaggiore (see Fig. 5b). The extent and pattern of the severe damage suggest a deep (> 10 km) and very large source that produced isotropic effects, which seemingly overrode local amplifications.

This epicentral zone includes the highest peak damage of the sequence. This fact may confirm that these catastrophic effects result from multiple events, as suggested by the spatio-temporal sequence we reconstructed.

*Source #**3** (Maiella – Gran Sasso)*

This area was affected by the 30 December shock. Historical evidence indicates that this event occurred either in the same date or in the days following the Isernia-Campobasso one (#**2**). The region is characterized by strong but poorly documented historical earthquakes (e.g. the 101 A.D., M 6.3 event) and by a largely uninhabited rugged mountain areas (with the highest peaks of the Apennines). The homogenous distribution of the VIII-IX and IX intensities in the region between the Maiella and Gran Sasso Mts. (Fig. 5a) and the distance from the area of source #**2** (Fig. 7) suggest that this event was caused by a deep source.

Estimates of earthquake magnitude

As earlier explained, one of the outputs of the Boxer code is the calculation of the moment magnitude. For the *macroseismic sources* being proposed in this study, we obtained the values of 6.9, 7.2 and 6.0, respectively for source #**1**, #**2** and #**3**. Considering the strongest earthquakes of the Italian catalog (Boschi et al., 2000), we notice that for source #**1** and, particularly, for source #**2** these values rank in the highest portion of the magnitude range.

The strongest single event known in the Italian catalog, the 28 Dec. 1908, Messina earthquake (M_w 7.1) was caused by a ~ 40 km long fault (Pino et al., 2000), similar to what was shown for the 23 Nov. 1980, Irpinia event (M_w 6.9; Pantosti and Valensise, 1990). In other words, the longest earthquake rupture ever observed in Italy does not appear to exceed 40 km. Based on geodynamic considerations, namely the extreme state of fragmentation of the lithosphere in peninsular Italy (Meletti et al., 2000; Oldow et al., 2002; Serpelloni et al., 2005), and on the historical reconstruction, we are led to believe that the maximum magnitude (and, therefore, size of earthquake faulting) of the 30 Dec. 1456 largest shock should be smaller than the M_w 7.2 derived from intensity data.

The current reference catalog of Italian seismicity (Gruppo di Lavoro CPTI, 2004) lists the 1456 sequence as two separate earthquakes on 5 and 30 December. The first event is the strongest, its magnitude being in the range M_w 7.1 (Boschi et al., 2000) to M_w 6.9 (Gruppo di Lavoro CPTI, 2004) (the scatter is due to slightly different magnitude computation algorithms, the data being the same), while the second event has a moment magnitude of 6.6 (Gruppo di Lavoro CPTI, 2004). In our study we have identified the contribution of the various shocks to the entire damage scenario. If (a) the associations presented here are correct and (b) the historical accounts do not lead to overestimated intensities, then the sum of the seismic moment of all events yields M_0 = 9.84E+19 Nm. This moment release corresponds to a single M_w 7.26 shock (i.e. 7.3), which would make 1456 the strongest known earthquake in peninsular Italy and the second strongest Italian earthquake after the 11 January 1693, eastern Sicily (M_w 7.4).

This conclusion raises an important issue concerning magnitude determinations and ranking of Italian earthquakes. A comparison between the mesoseismal areas of the 1456 and 1693 earthquakes (data for 1693 from: Boschi et al., 2000) shows that (a) the greatest distance between X-XI/XI datapoints is ~175 km vs. ~125, respectively; b) the X-XI mesoseismal area is ~3,800 vs. ~3,200 sq. km, respectively; and c) although clustered in three main groups, X and XI intensities for the 1456 sequence are very densely distributed across the central-southern Apennines. Conversely, the 1693 earthquake has two very distant areas of X-XI/XI damage, which suggests it is composed of two main events. Based on these simple arguments, we believe that the 1456 crisis ranks as the largest *event of seismic moment release within a short space and time interval* in Italian seismic history.

Similarly to 1456 and 1693, most catastrophic Italian earthquakes show evidence of complex and/or multiple sources (Westaway, 1987; Westaway and Jackson, 1987; Bernard and Zollo, 1989; Porfido et al., 2002; Castelli et al., 2005; Vallée and Di Luccio, 2005). Current methods for parameterizing historical earthquakes from intensity data (e.g.: Gasperini et al., 1999) envelope

maximum intensity datapoints even if they cluster in more than one discrete group distant from one another, as is the case of the 1693 earthquake. In addition, magnitude estimates tend to rely on medium intensity datapoints (in the case of the 1456, VI-VIII), which are usually incomplete for old historical earthquakes. Because of these circumstances, the resulting moment magnitude can be highly unreliable and may bias catalog information in the magnitude range that is most critical to constrain earthquake rates and, hence, assess seismic hazard.

Seismogenic sources of the 1456 events

Constraints from geological and tectonic observations and models

The *macroseismic sources* proposed in the previous chapter are based solely on the analysis of the intensity data in Table 2, using the algorithm by Gasperini et al. (1999). As we have previously discussed, however, such data may contain descriptions of cumulative damage from multiple events and therefore may overestimate intensities for individual earthquakes. The lack or uneven distribution of intermediate level intensities may lead the algorithm to an unstable solution for source strike. To develop a physically consistent source for the three main events (see Fig. 8), we relied on the following geological constraints (in chronological order):

(i) among several others, Sella et al. (1988) and Sawyer (2001) use subsurface data to show that numerous fault systems disrupt the top of the Apulian platform beneath the Apennine edifice. These systems include a set of NW-SE trending, SW-dipping normal faults beneath the Candela-Bradano foredeep, and a set of near-vertical E-W trending faults, having various kinematics, beneath the Capitanata. These regional structures are present west and southwest of the Gargano

and extend to the west toward Isernia. Other E-W structures can be mapped from the Capitanata to inner Sannio and Matese, east of the Vulture volcano, and between Potenza and Matera. Some of these structures fall in the epicentral areas of the 1456 main events and some other earthquakes in the foreland;

(ii) paleoseismological data (Blumetti et al., 2000; Galli and Galadini, 2003) indicate that, although lying in a peak intensity area of source #**2** (Fig. 7), the NW-SE trending normal fault responsible for the 1805, Molise event (M_w 6.6) did not rupture in the 1456 earthquake. Such evidence dictates that a causative fault for the area of source #**2** must be sought to the east, that is to say toward the source area of the 31 October-1 November, 2002, Molise earthquakes;

(iii) among others, Chilovi et al. (2000) and Piccardi (2005) show evidence of the activity of the Mattinata Fault zone, which cuts across the Gargano from east to west. Most of the kinematic indicators provided by these authors suggest a right-lateral kinematics, the same shown by the focal mechanisms of the 31 October-1 November, 2002, Molise earthquakes, which occurred along strike ~30 km to the west;

(iv) Di Bucci et al. (2002) describe a set of active structures coalescing in the Carpino – Le Piane system in the Isernia area, that have orientation and kinematics similar to the faults shown in point (v). This active fault approximately borders the epicentral area of source #**2** to the west;

(v) Valensise and Pantosti (2001b) and DISS Working Group (2006, and references therein) describe a set of large northeast-dipping normal faults along the axis of the Southern Apennines (NW-SE trending), as the sources of the major dip-slip earthquakes of the region. These large faults represent the active extensional axis that is 25-50 km west of the Potenza 1990 and Molise 2002 earthquakes, respectively;

(vi) Di Bucci et al. (2006) use analog sandbox models to explore the geometric, kinematic and dynamic relationships between the Mattinata Fault zone and the Molise hinterland, by

investigating the effects of dextral strike-slip reactivation of a large pre-existing shear zone. In their model, these authors demonstrate that the deep right-lateral reactivation (based on the hypocentral depth from the Molise 2002 earthquakes) is transferred along strike from the foreland to the mountain belt equivalent. They also show how the reactivated deep shear zone generates ancillary fault systems and deformation partitioning in the lower crust beneath the mountain belt along a major, E-W trending, pre-existing lineament like the Mattinata Fault zone;

(vii) DISS Working Group (2006, and references therein) associates a number of strike-slip faults, roughly trending E-W at various latitudes between Campobasso and Potenza, with moderate to strong earthquakes in the Apulian domain. These seismogenic sources are located in the sector of the southern Apennines between the external part of the thrustbelt and the Apulian foreland.

Constraints from instrumental seismicity

As discussed earlier, nearly all earthquakes that occurred east of the main Apennines axis in the Apulian domain (i.e. the Gargano, Capitanata and Murge regions) do not reflect the extensional stress field that dominates the axial part of the mountain belt. In addition, the 16 July 1992, M_w 4.3 (event ID# 74 in Fig. 3) Guardiagrele earthquake struck a region about 25 km east of the northernmost epicentral area of 1456 (source #**3** in Fig. 7). The 1992 event occurred on the eastern slope of the Maiella Mt. at an hypocentral depth of 18-22 km and was caused by right-lateral slip on a subvertical E-W plane (or left-lateral slip on a subvertical N-S plane; Fig. 3; data from: Frepoli and Amato, 2000). This region is bordered by the mesoseismal areas of the 1881-1882 Lanciano-Chieti (M_w ~5.0, # 39-40) and the larger 1706 Maiella (M_w 6.6, # 23) and 1933 Lama dei Peligni (M_w 6.1, # 53) earthquakes (Fig. 3).

In other words, the piedmont region that extends from the southern portion of the Maiella Mt. to the Chieti-Pescara area to the northeast is the locus of key earthquakes located east of the main axis

of the Apennines; a similar case to that of the 2002 Molise (# 76-77) and 1990 Potenza (# 72) earthquakes toward the south. We believe that seismicity in this region is somehow linked to that of the E-W trending Tremiti Line and the northern epicentral zone of the 1456 sequence (source #**3**; Fig. 6). Based on the 18-22 km hypocentral depth of the 1992 event, we suggest that in this area, earthquakes of moderate magnitude with right-lateral E-W focal mechanisms are confined to the deep portion of the seismogenic layer. As stated at the beginning, similar geometry and kinematics is known also for the 1971 Monteleone (# 62; Fig. 3), 1990-1991 Potenza (# 72-73) and 2002 Molise earthquakes (#76-77). In particular, the deep nature of E-W faulting is effectively demonstrated by a comparison between the 1980 Irpinia sequence, occurring at a depth of 5-13 km (Amato and Selvaggi, 1993), and the 1990-1991 Potenza aftershocks, occurring in the 14-23 km depth range (Ekström, 1994) and ca. 30 km east of the crustal volume affected by the 1980 Irpinia sequence. New data from Chiarabba et al. (2005) confirm that the seismogenic layer deepens eastward from the Apennines to the foreland.

In synthesis:

a) E-W trending dextral strike-slip earthquake sources are present at deeper crustal levels in the southern Apennines whereas major dip-slip sources are present at shallower depths;
b) Such active faults are located east of the Apennines backbone, and may be present throughout the entire Apulian foreland.

Seismogenic faults of the mainshocks

Having (i) characterized the historical and instrumental seismicity framework, (ii) defined the time-and-space distribution of damage areas, and (iii) summarized major tectonic and seismicity constraints, we propose a model for the three seismogenic faults responsible for the primary shocks

(hereafter *seismogenic sources*, labeled ***A***, ***B*** and ***C***; Fig. 8). These *seismogenic sources* are the geological equivalent of the *macroseismic sources* in Fig. 7; both types of sources are in the same chronological order of occurrence, so that source ***A*** corresponds to source #**1**, etc.

The Maiella – Gran Sasso area (#**3** in Fig. 7, ***C*** in Fig. 8) was struck only by one large event, whereas the larger damage areas of Piana Campana etc. and Matese – Gargano (#**1** and #**2** in Fig. 7, ***A*** and ***B*** in Fig. 8) almost certainly reflect the effects of multiple events. Therefore, our estimates for the size and location of these latter sources (parameters listed in Fig. 8) are based on the crustal volume where seismogenic faulting is thought to have occurred during the major events, rather than the magnitude obtained from the macroseismic data.

The following scheme summarizes how we constrained the various source parameters:

- Moment magnitude (M_w): for source ***C***, M_w is the same one obtained from macroseismic data using the Gasperini et al. (1999) procedure. As for sources ***A*** and ***B***, M_w is lower than that derived from the automatic procedure, likely due to damage overestimation and constraints imposed by empirical and analytical scaling laws;
- Source location: for source ***C***, the location reflects the epicenter shown in Fig. 7. Regarding sources ***A*** and ***B***, locations are constrained by the presence of adjoining known seismogenic faults (DISS Working Group, 2006, and references therein);
- Fault dimensions: these derive from the previous section, unless adjoining known seismogenic faults dictated upper size limits;
- Maximum slip: as far as the ***A*** and ***B*** sources (that caused the strongest events), we assume them to be 1.1 and 2.5 m, respectively, based on maximum slip per event measured for destructive earthquakes in the region, i.e. the 23 Nov 1980, Irpinia (M 6.9, ID # 68; data in Pantosti et al., 1993) and the 13 Jan 1915, Marsica (M 7.0, # 49; data in Amoruso and Crescentini, 1998); for the

C source we chose a smaller value, based on the same principle. All values obey the Kanamori and Anderson (1975) analytical relationships;

- Top and bottom depth: these values are based on instrumental data from the Monteleone 1971 and Molise 2002 earthquakes (in the depth range 11 to 25 km: Pondrelli et al., 2003; Chiarabba et al., 2005) adjacent to sources ***A*** and ***B***.
- Strike, dip, rake: strike is based on the seismicity trends (see Fig. 3), published sources (Vallée and Di Luccio, 2005; DISS Working Group, 2006) for the Molise 2002 (M 5.8) events, and on large known E-W trending structures in the subsurface (Sella et al., 1988; Sawyer, 2001); dip and rake correspond to values for the 1930 Irpinia earthquake (ID # 51, M 6.7; Jimenez, 1991; Ferrari et al. 2002).

The sum of all individual seismic moments is M_0 = 6.84E+19 Nm. Similarly to what we discussed for the *macroseismic sources*, the corresponding moment magnitude would be M_w = 7.15, if this moment were released in a single large earthquake.

A) Ariano Irpino (Sannio)

Source ***A*** has the potential to generate a M_w = 6.9 earthquake, which would be consistent with the effects of the large 5 December mainshock and those of the first part of the 1456 sequence. We propose oblique right-lateral slip on a WSW-ENE striking fault to explain the maximum damage toward the inner thrustbelt and to the east (along strike). Source ***A*** is bordered by faults that caused the 1688 (ID # 20) and 1732 (ID # 28) earthquakes to the west and by the causative fault of the 1361 event (ID # 9) to the east (DISS Working Group, 2006, and references therein).

B) Frosolone (north of Matese)

Source ***B*** caused the largest cumulative damage of the sequence. Taking into account a single mainshock and the constraints from adjoining seismogenic faults, this source shows rather conservative dimensions compared to those derived from the treatment of intensity data using Boxer. We hypothesize a WSW-ENE fault with oblique right-lateral slip and M_w = 7.0, corresponding to the largest event of 30 December. This fault is bordered by the NW-SE trending Carpino – Le Piane active structure shown by Di Bucci et al. (2002) to the west and by the source of the 1 November 2002 Molise earthquake (ID # 77) shown by Valensise et al. (2004), Vallée and Di Luccio (2005) and DISS Working Group (2006) to the east. Source ***B*** could explain the damage concentration near Isernia and Boiano and towards the sector northeast of Campobasso. The location of our proposed source is along the main E-W seismic alignment defined by the 2002 Molise sequence (ID #76, 77), the 1627 Capitanata earthquake (ID # 17), and the active Mattinata Fault system, including the 1975, 1995 and 2006 events (ID # 64, 75 and 99, respectively) that exhibit E-W trending right-lateral focal solutions.

C) Tocco Casauria (northwestern Maiella)

The smallest by magnitude, source ***C*** is located near Tocco Casauria, at the northwestern lower flank of the Maiella Mt. We hypothesize oblique right-lateral slip and M_w = 6.0 for this E-W fault. The source could explain damage reported in the Sulmona Basin and in the eastern and southern coast borders of the Maiella. Source ***C*** is bordered by the Sulmona seismogenic fault (Valensise and Pantosti, 2001b; DISS Working Group, 2006) and the poorly constrained 101 A.D., San Valentino earthquake (ID # 2, listed as an M_w 6.3 in the reference catalog) to the west. The deep 1992, M_w 4.3 Guardiagrele earthquake (ID # 74), plausibly caused by right-lateral slip on an E-W fault, lies to the east of source ***C*** just across the Maiella Mt.

The seismogenic sources being proposed are located between the main extensional axis of the southern Apennines to the west and its outer front to the east. While the 1990 Potenza and the 2002 Molise earthquakes (all of them M_w 5.8) indicate pure right-lateral slip on E-W faults at depth near the external front of the southern Apennines, the focal mechanism for the destructive 1930 Irpinia earthquake (M_w 6.7) indicates normal faulting with a dextral component of motion along a ~E-W plane and is located closer to the extensional axis in the core of the belt. In their turn, (i) macroseismic patterns of large historical events and the seismogenic sources derived from them, (ii) well constrained right-lateral focal solutions on deep E-W planes, and (iii) the presence of large pre-existing E-W fault systems, all suggest that the seismicity east of the buried external front of the chain is caused by right-lateral reactivation of deeper E-W faults.

Conclusions

In the absence of positively identified earthquake sources, seismotectonic models of the southern Apennines generally assumed that the 1456 earthquake had ruptured several ~NW-SE trending normal fault segments similar to those responsible for the better known shallower earthquakes of the Southern Apennines (Magri and Molin, 1983; Meletti et al., 1988; Cecić et al., 1996; Troise et al., 1998; Teramo et al., 1999). On the grounds of (a) a new time-and-space analysis of the earthquake events, (b) instrumental evidence from significant adjoining earthquakes and (c) the presence of deep-seated regional ~E-W structures, we suggest that these multiple events were generated and/or controlled by oblique right-lateral reactivation of discrete segments of regional deeper, E-W seismogenic faults in a cascade fashion.

The unusual extent of the damage resulting from the 1456 sequence can be explained by (1) source multiplicity (i.e. combination of the shaking effects of faulting on three or more parallel ~E-W

strands), (2) depth of the sources that we interpret to be consistently below 10 km (implying a strong regional propagation), and (3) dynamic relation with large tectonic units of the Southern Apennines. While destructive (M_w > 6.5) earthquake activity in the core of the thrustbelt occurs within the uppermost 10-12 km of the crust, the proposed sources activated by the 1456 events likely ruptured the lower portion of the seismogenic layer (roughly between 10 and 25 km).

We propose that a seismogenic region, characterized by oblique dextral slip on ~E-W trending planes, dominates the structural domain bounded by the NW-SE trending system of main extensional faults (to the west) and the buried external Apennine front (to the east). Such sources are capable of generating destructive earthquakes (as demonstrated by the M_w 6.7, 1930 Irpinia earthquake) and would thus represent the western expression of roughly E-W oriented seismicity alignments marked by the earthquakes of intermediate magnitude (5.5 < M_w < 6.3) that occurred in the Apulian foreland.

Our hypothesis invokes stress interaction among multiple sources falling within neighboring domains. Such interaction has been observed either at the very short or long time scale (like the 1980 Irpinia sequence or the relationships between this earthquake and the 1990/1991 Potenza sequence; Troise et al., 1998). We believe that the 1456 seismic crisis, made of multiple destructive events across a uniquely wide area within a 30-45 day timespan, may represent a similar example of a triggering among large events occurring in the deeper Adriatic crust.

Based on the broader results of this work, we identified a zone of E-W trending seismicity further south that includes the 5 May 1990, M_w 5.8 Potenza earthquake, with right-lateral strike-slip kinematics, and a swath of smaller events aligned ~E-W that extends toward the southeastern tip of Apulia. The nature, regional extent and geodynamic implications of the overall E-W system highlighted in this work form the core of a broader ongoing research.

Acknowledgements

UF wishes to thank GV, his supervisor and co-author of this work, for his constant guidance and patience. The thorough reviews by A. Crone and A. Meltzner were greatly beneficial to the final version of this manuscript. We thank R. Basili, P. Burrato, D. Di Bucci, L. Improta, P. Vannoli and G. Ventura for fruitful discussions and support. Work supported by MIUR (Italy's Ministry for University and Research) FISR project "Diagnostica e salvaguardia di manufatti architettonici con particolare riferimento agli effetti derivanti da eventi sismici ed altre calamità naturali" (PI: A. Rovelli).

References

Alessio, G., C. Godano, and A. Gorini (1990). A Low Magnitude Seismic Sequence Near Isernia (Molise, Central Italy) in January 1986, *Pure Appl. Geophys.* **134**, 243-260.

Alessio, G., E. Esposito, A. Gorini, and S. Porfido (1995). Detailed study of the Potentino seismic zone in the Southern Apennines, Italy, *Tectonophysics* **250**, 113-134.

Amato, A., and G. Selvaggi (1993). Aftershock location and *P*-velocity structure in the epicentral region of the 1980 Irpinia earthquake, *Ann. Geophys.* **36**, 3-15.

Amoruso, A., L. Crescentini, and R. Scarpa (1998). Inversion of source parameters from near- and far-field observations: an application to the 1915 Fucino earthquake, central Apennines, Italy, *J. Geophys. Res.* **103**, 29,989-29,999

Ascione, A., A. Cinque, L. Improta, and F. Villani (2003). Late Quaternary faulting within the Southern Apennines seismic belt: new data from Mt. Marzano area (Southern Italy), *Quatern. Int.* **101/102**, 27–41.

Azzara, R., A. Basili, L. Beranzoli, C. Chiarabba, R. Di Giovambattista, and G. Selvaggi (1993). The seismic sequence of Potenza (May 1990), *Ann. Geophys.* **36**, 237-243.

Bernard, P., and A. Zollo (1989). The Irpinia Italy 1980 earthquake: detailed analysis of a complex normal fault, *J. Geophys. Res*. **94**, 1631-1648.

Blumetti, A.M., M. Caciagli, D. Di Bucci, L. Guerrieri, A.M. Michetti, and G. Naso (2000). Evidenze di fagliazione superficiale Olocenica nel Bacino di Boiano (Molise), Procs., 19º Meeting G.N.G.T.S., 1-9.

Boschi, E., G. Ferrari, P. Gasperini, E. Guidoboni, G. Smriglio and G. Valensise (1995). Catalogo dei forti terremoti in Italia dal 461 a.C. al 1980, ING-SGA, Bologna, with CD-Rom, 973 pp.

Boschi, E., E. Guidoboni, G. Ferrari, P. Gasperini, and G. Valensise (1997). Catalogo dei forti terremoti in Italia dal 461 a.C. al 1990, ING-SGA, Bologna, with CD-Rom, 644 pp.

Boschi, E., E. Guidoboni, G. Ferrari, D. Mariotti, G. Valensise, and P. Gasperini (eds.) (2000). Catalogue of strong italian earthquakes from 461 B.C. to 1997, *Ann. Geophys*. **43**, with CD-Rom, 259 pp.

Boschi, E., D. Pantosti, D. Slejko, M. Stucchi, and G. Valensise (eds.) (1993). Proceedings of the meeting "Irpinia ten years on", Sorrento 19-24 November 1990, *Ann. Geophys*. **36**, 353 pp.

Bottari A., B. Federico, L. Giovani, E. Lo Giudice, M.C. Spadea, and M. Vecchi (1981). Il terremoto irpino del 23 novembre 1980: il campo macrosismico e l'attenuazione dell'intensità, *Rend. Soc. Geol. It*. **4**, 549-551.

Butler, R.W.H., S. Mazzoli, S. Corrado, M. De Donatis, D. Di Bucci, R. Gambini, G. Naso, C. Nicolai, D. Scrocca, P. Shiner, and V. Zucconi (2004). Applying Thick-skinned Tectonic Models to the Apennine Thrust Belt of Italy: Limitations and Implications, in: K.R. McClay (ed.), Thrust tectonics (TT99), *Am. Ass. Petrol. Geol. Mem*. **82**, 647-667.

Carlson, R.E., and T.A. Foley (1992). Interpolation of Track Data with Radial Basis Methods, *Comput. Math. Appl*. **24**, 27-34.

Castello, B., Selvaggi, G., Chiarabba, C., and Amato, A. (2006). CSI Catalogo della sismicità italiana 1981-2002, versione 1.1, INGV-CNT, Roma, http://www.ingv.it/CSI/.

Castelli, V., R. Camassi, and P. Galli (2005). 1561: quanti terremoti e quante faglie? Procs. 24° Meeting G.N.G.T.S, Rome, 13-14.

Cecić, N., R.M.W. Musson, and M. Stucchi (1996). Do seismologists agree upon epicentre determination from macroseismic data?, *Ann. Geophys.* **39**, 1013-1027.

Chiarabba, C., P. De Gori, L. Chiaraluce, P. Bordoni, M. Cattaneo, M. De Martin, A. Frepoli, A. Michelini, A. Monachesi, M. Moretti, G.P. Augliera, E. D'Alema, M. Frapiccini, A. Gassi, S. Marzorati, P. Di Bartolomeo, S. Gentile, A. Govoni, L. Lovisa, M. Romanelli, G. Ferretti, M. Pasta, D. Spallarossa, and E. Zunino (2005). Mainshocks and aftershocks of the 2002 Molise seismic sequence, southern Italy, *J. Seismol*., **9**, 487-494.

Chiarabba, C., L. Jovane, and R. Di Stefano (2005). A new view of Italian seismicity using 20 years of instrumental recordings, *Tectonophysics* **395**, 251-268, doi: 10.1016/j.tecto.2004.09.013.

Chiaruttini, C., and L. Siro (1991). Focal mechanism of an earthquake of Baroque age in the "Regno delle Due Sicilie" (Southern Italy), *Tectonophysics* **193**, 195-203.

Chilovi, C., A.J. De Feyter, and A. Pompucci (2000). Wrench zone reactivation in the Adriatic Block: the example of the Mattinata Fault System (SE Italy), *Boll. Soc. Geol. It*. **119**, 3-8.

Cocco, M., C. Chiarabba, M. Di Bona, G. Selvaggi, L. Margheriti, A. Frepoli, F.P. Lucente, A. Basili, D. Jongmans, and M. Campillo (1999). The April 1996 Irpinia seismic sequence: Evidence for fault interaction, *J. Seismol*. **3**, 105-117.

Cozzetto, F. (1986). Mezzogiorno e demografia nel XV secolo, Rubbettino Ed., Soveria Mannelli (CZ), 212 pp.

D'Agostino, N., and G. Selvaggi (2004). Crustal motion along the Eurasia-Nubia plate boundary in the Calabrian Arc and Sicily and active extension in the Messina Straits from GPS measurements, *J. Geoph. Res.* **109**, B11402, doi: 10.1029/2004JB002998.

Del Gaudio, V., P. Pierri, G. Calcagnile, and N. Venisti (2005). Characteristics of the low energy seismicity of central apulia (Southern Italy) and hazard implications, *J. Seismol*. **9**, 39-59, doi: 10.1007/s10950-005-1593-9.

Deschamps, A., and G.C.P. King (1984). Aftershocks of the Campania-Lucania (Italy) earthquake of 23 November 1980, *B. Seismol. Soc. Am*. **74**, 2483-2517.

Di Bucci, D., S. Corrado, and G. Naso (2002). Active faults at the boundary between Central and Southern Apennines (Isernia, Italy), *Tectonophysics* **359**, 47-63.

Di Bucci, D., and S. Mazzoli (2003). The October-November 2002 Molise seismic sequence (southern Italy): an expression of Adria intraplate deformation, *J. Geol. Soc. London* **160**, 503-506.

Di Bucci, D., A. Ravaglia, S. Seno, G. Toscani, U. Fracassi, and G. Valensise (2006). Seismotectonics of the Southern Apennines and Adriatic foreland: insights on active regional E-W shear zones from analogue modeling, *Tectonics* **25**, TC4015, doi: 10.1029/2005TC001898.

DISS Working Group (2006). Database of Individual Seismogenic Sources (DISS), Version 3.0.2: A compilation of potential sources for earthquakes larger than M 5.5 in Italy and surrounding areas. http://www.ingv.it/DISS/, © INGV 2005, 2006 - Istituto Nazionale di Geofisica e Vulcanologia - All rights reserved.

Ekström, G. (1994). Teleseismic analysis of the 1990 and 1991 earthquakes near Potenza, *Ann. Geofis*. **37**, 1591-1599.

Emolo, A., G. Iannaccone, A. Zollo, and A. Gorini (2004). Inferences on the source mechanisms of the 1930 Irpinia (Southern Italy) earthquake from simulations of the kinematic rupture process, *Annals Geophys*. **47**, 1743-1754.

Ferrari, G., A. Megna, A. Nardi, B. Palombo, B. Perniola, and N.A. Pino (2002). The 1930 Irpinia earthquake; collection and analysis of historical waveforms, *Eos* **83**, 47, 1045.

Fracassi, U., B. Niviére, and T. Winter (2005). First appraisal to define prospective seismogenic sources from historical earthquake damages in southern Upper Rhine Graben, *Quat. Sc. Rev*. **24**, 401-423, doi: 10.1016/j.quascirev.2004.05.009.

Fracassi, U., and G. Valensise (2004). The "layered" seismicity of Irpinia: important but incomplete lessons learned from the 23 November 1980 earthquake, in: M. Pecce, G. Manfredi, A. Zollo (eds.), The many facets of seismic risk, CRdC-AMRA, 46-52.

Frepoli, A., and A. Amato (2000). Fault plane solutions of crustal earthquakes in Southern Italy (1988-1995): seismotectonic implications, *Ann. Geophys*. **43,** 437-467.

Galli, P., and F. Galadini (2003). Disruptive earthquakes revealed by faulted archaelogical relics in Samnium (Molise, southern Italy), *Geophys. Res. Lett*. **30**, doi: 10.1029/2002GL016456.

Galli, P., and D. Molin (2004). Macroseismic Survey of the 2002 Molise, Italy, Earthquake and Historical Seismicity of San Giuliano di Puglia, *Earthq. Spectra* **20**, S39–S52.

Gasparini, C., G. Iannaccone, and R. Scarpa (1985). Fault-plane solutions and seismicity of the Italian peninsula, *Tectonophysics* **117**, 59-78.

Gasperini, P., F. Bernardini, G. Valensise, and E. Boschi (1999). Defining Seismogenic Sources from Historical Earthquake Felt Reports, *B. Seismol. Soc. Am*. **89**, 94-110.

Giardini, D. (1993). Teleseismic observation of the November 23 1980, Irpinia earthquake, *Ann. Geophys*. **36**, 17-25.

Gruppo di Lavoro CPTI (2004). Catalogo Parametrico dei Terremoti Italiani, versione 2004 (CPTI04), INGV, http://emidius.mi.ingv.it/CPTI/.

Gruppo di Lavoro MPS (2004). Redazione della mappa di pericolosità sismica prevista dall'Ordinanza PCM 3274 del 20 marzo 2003. Rapporto Conclusivo per il Dipartimento della Protezione Civile. INGV, Milano-Roma, 65 pp. + 5 appendixes, http://zonesismiche.mi.ingv.it/.

Guidoboni, E., and A. Comastri (2005). Catalogue of earthquakes and tsunamis in the Mediterranean area from the 11th to the 15th century, Istituto Nazionale di Geofisica e Vulcanologia – SGA, Bologna, 1037 pp.

Guidoboni, E. and G. Ferrari (2004). Integrazione di ricerca di archeologia e storia territoriale riguardante il terremoto del 1456 e l'area molisano-campana relativamente ai terremoti prima del Mille, RPT 255/03, SGA – Storia Geofisica Ambiente, Bologna, 139 pp.

Harvard Univ. (2005). Harvard Centroid-Moment Tensor Project, http://www.seismology.harvard.edu/projects/CMT/.

Hippolyte, J.C., J. Angelier, and F. Roure (1994). A major geodynamic change revealed by Quaternary stress patterns in the Southern Apennines (Italy), *Tectonophysics* **230**, 199-210.

Improta, L., M. Bonagura, P. Capuano, and G. Iannaccone (2003). An integrated geophysical investigation of the upper crust in the epicentral area of the 1980, Ms=6.9, Irpinia earthquake (Southern Italy), *Tectonophysics* **361**, 139–169.

Jiménez, E. (1991). Focal mechanism of some european earthquakes from the analysis of single station long-periods record, in: J. Mezcua, A. Udías (eds.), Seismicity, Seismotectonics and Seismic Risk of the Ibero-Maghrebian Region, *I.G.N. Série Monografía* **8**, 87-96.

Kanamori, H., and D.L. Anderson (1975). Theoretical basis of some empirical relations in seismology, *B. Seismol. Soc. Am.*, **65**, 1073-1095.

Louvari, E.K., and A.A. Kiratzi (2000). The Focal Mechanism of the April 26, 1988 (Mw 5.3) Earthquake (Adriatic Sea), in: I. Panayides, C. Xenophontos, J. Malpas (eds.), 3rd International Conference on the Geology of the Eastern Mediterranean Procs., 147-158.

Magri, G., and D. Molin (1983). Il terremoto del dicembre 1456 nell'Appennino centro-meridionale, ENEA, RT/AMB 83/08, 180 p.

Maschio, L., L. Ferranti, and P. Burrato (2005). Active extension in Val d'Agri area, Southern Apennines, Italy: implications for the geometry of the seismogenic belt, *Geophys. J. Intern*. **162**, 591-609, doi: 10.1111/j.1365-246X.2005.02597.x.

Mazzoli, S., and M. Helman (1994). Neogene patterns of relative plate motion for Africa-Europe: Some implications for recent Mediterranean tectonics, *Geol. Rundsch*. **83**, 464-468.

MEDNET (2006). MEDiterranean Very Broadband Seismographic NETwork, INGV, http://mednet.rm.ingv.it/events/Welcome.html.

Mele, G. (2001). The adriatic lithosphere is a promontory of the African plate: Evidence of a continuous mantle lid in the Ionian Sea from efficient Sn propagation, *Geophys. Res. Lett*. **28**, 431–434, doi: 10.1029/2000GL012148.

Mele, G., A. Rovelli, D. Seber, and M. Barazangi (1996). Lateral variations of Pn propagation in Italy: Evidence for a high-attenuation zone beneath the Apennines, *Geophys. Res. Lett.* **23**, 709-712, doi: 10.1029/96GL00480.

Meletti, C., E. Patacca, and P. Scandone (2000). Construction of a seismotectonic model: the case of Italy, *Pure Appl. Geophys*. **157**, 11–35, doi: 10.1007/PL00001089.

Meletti, C., E. Patacca, P. Scandone, and B. Figliuolo (1988). Il Terremoto del 1456 e la sua interpretazione nel quadro sismotettonico dell'Appennino Meridionale, in: B. Figliuolo (ed.), Il Terremoto del 1456, Osservatorio Vesuviano, Storia e Scienze della Terra, 71-108 (I) & 35-163 (II).

Menardi Noguera, A., and G. Rea (2000). Deep structure of the Campanian–Lucanian Arc (Southern Apennine, Italy), *Tectonophysics* **324**, 239–265.

Milano, G., R. Di Giovambattista, and G. Alessio (1999). Earthquake swarms in the Southern Apennines chain (Italy): the 1997 seismic sequence in the Sannio – Matese Mountains, *Tectonophysics* **306**, 57-78.

Milano, G., G. Ventura, and R. Di Giovambattista (2002). Seismic evidence of longitudinal extension in the Southern Apennines chain (Italy): The 1997-1998 Sannio–Matese seismic sequence, *Geophys. Res. Lett.* **29**, doi: 10.1029/2002GL015188.

Monachesi, G., and M. Stucchi (eds.) (1997). DOM4.1: Un database di osservazioni macrosismiche di terremoti di area italiana al di sopra della soglia del danno, Gruppo Naz. Difesa dai Terremoti, Milano-Macerata, http://emidius.mi.ingv.it/DOM.

Montone, P., M.T. Mariucci, S. Pondrelli, and A. Amato (2004). An improved stress map for Italy and surrounding regions (Central Mediterranean), *J. Geophys. Res*. **109**, doi: 10.1029/2003jb002703.

Mostardini, F., and S. Merlini (1986). Appennino centro-meridionale. Sezioni geologiche e proposta di modello strutturale, *Mem. Soc. Geol. It*. **35**, 177-202.

Oldow, J.S., L. Ferranti, D.S. Lewis, J.K. Campbell, B. D'Argenio, R. Catalano, G. Pappone, L. Carmignani, P. Conti, and C.L.V. Aiken (2002). Active fragmentation of Adria, the north African promontory, central Mediterranean orogen, *Geology* 30, 779 – 782, doi: 10.1130/0091-7613(2002)030<0779:AFOATN>2.0.CO;2

Pace, B., P. Boncio, and G. Lavecchia (2002). The 1984 Abruzzo earthquake (Italy): an example of seismogenic process controlled by interaction between differently oriented synkinematic faults, *Tectonophysics* **350**, 237-254.

Pantosti, D., D.P. Schwartz, and G. Valensise (1993). Paleoseismology along the 1980 surface rupture of the Irpinia fault: implications for earthquake recurrence in the southern Apennines, Italy, *J. Geophys. Res*. **98**, 6,561-6,577.

Pantosti, D., and G. Valensise (1988). La faglia sud-appenninica: identificazione oggettiva di un lineamento sismogenetico nell'Appennino meridionale, Procs. 7° Meeting G.N.G.T.S, Rome, 205-220.

Pantosti, D., and G. Valensise (1990). Faulting mechanism and complexity of the 23 November, 1980, Campania-Lucania earthquake inferred form surface observations, *J. Geophys. Res*. **95**, 15,319-15,341.

Panza, G.F., A. Craglietto, and P. Suhadolc (1991). Source geometry of historical events retrieved by synthetic isoseismals, *Tectonophysics* **193**, 173-184.

Patacca, E., and P. Scandone (1989). Post-Tortonian mountain building in the Apennines. The role of the passive sinking of a relict lithospheric slab, in A. Boriani, M. Bonafede, G.B. Piccardo, G.B. Vai (eds.), The Lithosphere in Italy, *Atti Accad. Naz. Lincei*, Roma, **80**, 157-176.

Piccardi, L. (2005). Paleoseismic evidence of legendary earthquakes: The apparition of Archangel Michael at Monte Sant'Angelo (Italy), *Tectonophysics* **408**, 113–128, doi: 10.1016/j.tecto.2005.05.041.

Pino, N.A., D. Giardini, and E. Boschi (2000). The December 28, 1908, Messina Straits, southern Italy, earthquake: Waveform modeling of regional seismograms, *J. Geophys. Res*. **105** (B11), 25,473-25,492.

Pondrelli, S., F. Di Luccio, E. Fukuyama, S. Mazza, M. Olivieri, and N.A. Pino (2003). Fast determination of moment tensors for the recent Molise (southern Italy) seismic sequence, *ORFEUS Newsl*. **5**.

Porfido, S., E. Esposito, E. Vittori, G. Tranfaglia, A.M. Michetti, M. Blumetti, L. Ferreli, L. Guerrieri, and L. Serva (2002). Areal distribution of ground effects induced by strong earthquakes in the Southern Apennines (Italy), *Surv. Geophys.* **23**, 529-562.

Riguzzi, F. (1999). Intensity Field of the 19 June 1975 Gargano (Southern Italy) Earthquake, *Phys. Chem. Earth Pt. A* **24**, 489-493.

Sawyer, R.K. (2001). An Integrated Surface and Subsurface Interpretation of the Stratigraphy, Structure and Tectonics of the Southcentral Apennines of Italy, *Amer. Assoc. Petrol. Geol. Bull.* **85**, suppl.

Schweizerischer Erdbebendienst (SED) Swiss Seismological Service (2005). Moment Tensor Catalogue, http://www.seismo.ethz.ch/mt/.

Sella, M., C. Turci, and A. Riva (1988). Sintesi geopetrolifera della Fossa Bradanica (avanfossa della Catena Appenninica meridionale), *Mem. Soc. Geol. It.* **41**, 87-107.

Serpelloni, E., M. Anzidei, P. Baldi, G. Casula, and A. Galvani (2005). Crustal velocity and strainrate fields in Italy and surrounding regions: new results from the analysis of permanent and non-permanent GPS networks, *Geophys. J. Int.* **161**, 861-880, doi: 10.1111/j.1365-246X.2005.02618.x.

Serpelloni, E., M. Anzidei, P. Baldi, G. Casula, and A. Galvani (2006). GPS measurements of active strains across the Apennines (Italy), *Annals. Geoph.* **49**, 319-329.

Teramo, A., E. Stillitani, A. Bottari, and D. Termini (1999). The December 5th, 1456 Central Italy Earthquake: A Discussion of a Possible Reshaping of Intensity Distribution by Vectorial Modelling, *Pure Appl. Geophys*. **155**, 131–148.

Tertulliani, A., M. Anzidei, A. Maramai, M. Murru, and F. Riguzzi (1992). Macroseismic Study of the Potenza (Southern Italy) Earthquake of 5 May 1990, *Nat. Hazards* **6**, 25-38.

Troise, C., G. De Natale, F. Pingue, and S.M. Petrazzuoli (1998). Evidence for static stress interaction among earthquakes in the south-central Apennines (Italy), *Geophys. J. Int*. **134**, 809-817.

Valensise, G., and D. Pantosti (2001a). The investigation of potential earthquake sources in peninsular Italy: A review, *J. Seismol.* **5**, 287-306.

Valensise, G., and D. Pantosti (eds.) (2001b). Database of Potential Sources for Earthquakes Larger than M 5.5 in Italy, *Ann. Geophys*. **44**, Suppl. 1, with CD-Rom.

Valensise, G., D. Pantosti, and R. Basili (2004). Seismology and Tectonic Setting of the Molise Earthquake Sequence of October 31-November 1, 2002, *Earthq. Spectra* **20**, S23-S37.

Vallée, M., and F. Di Luccio (2005). Source analysis of the 2002 Molise, southern Italy, twin earthquakes (10/31 and 11/01), *Geophys. Res. Lett*. **32**, doi: 10.1029/2005GL022687.

Vannucci, G., and G. Gasperini (2004). The new release of the Database of Earthquake Mechanisms of the Mediterranean Area (EMMA version 2), *Ann. Geophys*. **47**, suppl. 1, with CD-Rom.

Viti, A. (1972). Note di diplomatica ecclesiastica sulla contea di Molise dalle fonti delle pergamene capitolari di Isernia. Città e diocesi dall'eta longobarda alla aragonese, Arte Tipografica, Napoli, 385 pp.

Wells, D.L., and K.J. Coppersmith (1994). New Empirical Relationships among Magnitude, Rupture Length, Rupture Width, Rupture Area, and Surface Displacement, *B. Seismol. Soc. Am*., **84**, 974-1002.

Westaway, R. (1987). The Campania, southern Italy, earthquakes of 1962 August 21, *Geophys. J. R. Astr. Soc.* **88**, 1-24.

Westaway, R., R. Gawthorpe, and M. Tozzi (1989). Seismological and field observations of the 1984 Lazio-Abruzzo earthquakes; implications for the active tectonics of Italy, *Geophys. J. R. Astr. Soc.* **98**, 489-514.

Westaway, R., and J. Jackson (1987). The earthquake of 1980 November 23 in Campania-Basilicata (southern Italy), *Geophys. J. R. Astr. Soc*. **90**, 375-443.

Istituto Nazionale di Geofisica e Vulcanologia, Via di Vigna Murata 605, 00143 Roma, Italy

fracassi@ingv.it, valensise@ingv.it

Historical and instrumental earthquakes

Historical earthquakes

ID	Date	Time (local)	Lat	Lon	M_w	Data n.	Imax (MCS)	Reference	Location	Source
1	0099 -	-	41.350	14.800	6.3	1	IX-X	BO00, CPTI	Circello	
2	0101 -	-	42.230	13.980	6.3	1	IX-X	BO00, CPTI	San Valentino	
3	0848 06 -	-	41.480	14.270	6.0	5	IX	BO00, CPTI	Matese	
4	0989 10 25	-	41.020	15.170	6.0	10	IX-X	BO00, CPTI	Irpinia	
5	1125 10 11	-	41.600	15.000	5.7	4	IX	BO00, CPTI	Sannio - Molise	
6	1223 -	-	41.850	16.030	6.0	5	IX	BO00, CPTI	Gargano	
7	1315 12 03	09:30	42.000	13.970	6.0	15	IX	BO00, CPTI	Central Italy	
8	1349 09 09	08:15	41.480	14.070	6.7	22	X	BO00, CPTI	Lazio - Molise	MS
9	1361 07 17	19:30	41.230	15.450	6.0	5	X	BO00, CPTI	Ascoli Satriano	GG
10	1414 -	-	41.800	16.180	5.8	1	VIII-IX	BO00, CPTI	Vieste	
11	1461 11 26	21:30	42.308	13.543	6.5	7	X	DOM, CPTI	Aquilano	
12	1456 12 05	-	41.302	14.711	7.0	199	X	BO00, CPTI	Molise	MS
13	1456 12 05	-	41.150	14.867	6.6	199	X	BO00, CPTI	Beneventano	MS
14	1466 01 15	02:00	40.765	15.334	6.1	31	VIII-IX	SGA	Irpinia	
15	1560 05 11	04:40	41.250	16.480	5.7	5	VIII	BO00, CPTI	Bisceglie	GG
16	1561 08 19	14:10	40.520	15.480	6.4	30	X	BO00, CPTI, CA05	Vallo di Diano	MS
17	1627 07 30	10:50	41.730	15.350	6.7	46	X	BO00, CPTI	Gargano	GG
18	1646 05 31	04:30	41.870	15.930	6.2	10	IX-X	BO00, CPTI	Gargano	
19	1654 07 23	00:25	41.630	13.680	6.2	44	X	BO00, CPTI	Sorano-Marsica	
20	1688 06 05	15:30	41.280	14.570	6.7	210	XI	BO00, CPTI	Sannio	GG
21	1694 09 08	11:40	40.880	15.350	6.9	249	XI	BO00, CPTI	Irpinia - Basilicata	MS
22	1702 03 14	05:00	41.120	14.980	6.3	35	X	BO00, CPTI	Sannio - Irpinia	MS
23	1706 11 03	13:00	42.080	14.080	6.6	97	IX-X	BO00, CPTI	Maiella	MS
24	1713 01 03	-	40.588	17.113	4.8	2	VI-VII	DOM, CPTI	Massafra	
25	1720 06 07	-	41.261	15.920	5.2	6	VI-VII	DOM, CPTI	Cerignola	
26	1731 03 20	03:00	41.270	15.750	6.3	45	IX	BO00, CPTI	Capitanata	GG
27	1731 10 17	-	41.178	15.990	5.2	4	VI-VII	DOM, CPTI	Canosa di Puglia	
28	1732 11 29	07:40	41.080	15.050	6.6	167	X-XI	BO00, CPTI	Irpinia	GG
29	1762 10 06	12:10	42.300	13.580	5.9	6	IX-X	BO00, CPTI	Aquilano	
30	1805 07 26	21:00	41.500	14.470	6.6	218	X	BO00, CPTI	Boiano	GG
31	1826 02 01	16:00	40.520	15.730	5.6	17	IX	BO00, CPTI	Basilicata	MS
32	1826 10 26	18:00	40.451	17.868	5.3	6	VI-VII	DOM, CPTI	Manduria	
33	1845 07 10	-	40.665	16.607	4.6	8	VI	DOM, CPTI	Matera	
34	1846 08 08	-	40.530	16.113	5.2	12	VI-VII	DOM, CPTI	Campomaggiore	
35	1851 08 14	13:20	40.950	15.670	6.3	101	X	BO00, CPTI	Melfi	GG
36	1853 04 09	09:12	40.820	15.220	5.9	47	IX	BO00, CPTI	Irpinia	MS
37	1857 12 16	21:15	40.350	15.850	7.0	324	XI	BO00, CPTI	Basilicata	GG
38	1875 12 06	-	41.689	15.677	6.1	92	VIII	DOM, CPTI	Gargano - Capitanata	MS
39	1881 09 10	07:30	42.230	14.280	5.6	28	VIII	BO00, CPTI	Lanciano	MS
40	1882 06 06	05:40	41.550	14.200	5.3	34	VII	BO00, CPTI	Matese	
41	1885 12 26	-	41.543	14.679	5.4	27	VII	DOM, CPTI	Campobasso	
42	1889 12 08	-	41.830	15.692	5.5	75	VII	DOM, CPTI	Apricena	MS
43	1892 06 06	-	42.156	15.520	5.0	10	VI-VII	DOM, CPTI	Tremiti Is.	
44	1893 08 10	20:52	41.750	16.080	5.4	27	VIII-IX	BO00, CPTI	Gargano	
45	1903 05 04	03:44	41.034	14.557	5.1	24	VII-VIII	DOM, CPTI	Valle Caudina	
46	1905 03 14	19:16	40.951	14.805	4.7	52	VI-VII	DOM, CPTI	Beneventano	
47	1910 06 07	02:04	40.900	15.420	5.8	321	IX	BO00, CPTI	Irpinia - Basilicata	MS
48	1913 10 04	18:26	41.513	14.716	5.4	171	VII-VIII	DOM, CPTI	Matese	
49	1915 01 13	06:52	41.980	13.650	7.0	860	XI	BO00	Marsica	GG
50	1925 09 24	13:33	41.720	14.180	5.4	46	VII	BO00	W Molise	
51	1930 07 23	23:00	41.050	15.370	6.7	500	X	BO00, CPTI	Irpinia	GG
52	1933 03 07	14:39	41.023	15.351	5.1	42	VI	CPTI	Bisaccia	
53	1933 09 26	03:33	42.050	14.180	6.1	315	VIII-IX	BO00, CPTI	Lama dei Peligni	MS
54	1936 07 31	05:46	41.783	14.108	4.2	8	VII	ISOS	Castel di Sangro	
55	1948 08 18	21:12	41.580	15.750	5.6	59	VII-VIII	BO00, CPTI	Gargano - Capitanata	MS
56	1950 09 05	04:08	42.516	13.657	5.7	134	VIII	DOM, CPTI	Gran Sasso	GG
57	1951 01 16	01:11	41.808	15.900	5.2	48	VII	DOM, CPTI	Gargano	
58	1956 01 09	00:44	40.570	16.366	4.8	32	VII	DOM, CPTI	Grassano	
59	1958 06 24	06:07	42.340	13.477	5.1	125	VII	DOM, CPTI	Aquilano	
60	1962 08 21	18:19	41.130	14.970	6.2	264	IX	BO00, CPTI	Irpinia	MS

61	1963 02 13	12:45	40.658	15.782	5.1	17	VII	DOM, CPTI	Tito	
62	1971 05 06	03:45	41.150	15.233	5.2	24	VII	INGV, CPTI	Monteleone	
63	1971 11 29	18:49	40.500	15.800	4.8	11	VI	DOM, CPTI	Marsico	
64	1975 06 19	10:11	41.650	15.730	5.0	61	VI-VII	DOM, RIG, CPTI	Gargano	
65	1979 06 04	10:10	41.840	15.600	5.0	-	VII	INGV	Gargano	
66	1980 04 23	11:11	40.480	13.480	4.6	-	-	INGV	Tyrrhenian Sea	
67	1980 05 14	01:41	40.360	15.770	5.0	-	VI	INGV	High Agri Valley	
68	1980 11 23	18:34	40.850	15.280	6.9	1056	X	BO00, CPTI	Irpinia - Basilicata	GG
69	1981 02 14	17:27	40.985	14.613	4.9	83	VII-VIII	INGV, CPTI	Baiano	
70	1984 05 07	17:49	41.670	14.057	5.9	837	VIII	BO00, CPTI	Abruzzo	GG
71	1986 07 23	08:19	40.626	15.705	4.6	48	VI	CPTI	Potentino	
72	1990 05 05	07:21	40.640	15.860	5.8	628	VII-VIII	INGV, TERT, CPTI	Potenza	GG
73	1991 05 26	12:25	40.668	15.803	5.2	288	VII	INGV, CPTI	Potenza	
74	1992 07 16	05:38	42.110	14.110	4.3	43	VI	INGV, FA0A	Guardiagrele	
75	1995 09 30	10:14	41.754	15.656	5.2	91	VI	INGV, CPTI	Gargano	
76	2002 10 31	10:32	41.630	14.770	5.8	51	VIII-IX	INGV, CPTI, VALL	Molise	GG
77	2002 11 01	15:09	41.680	14.990	5.8	31	VIII-IX	GA04, CPTI, VALL	Molise	GG

Instrumental earthquakes

ID	*Date*	*Time (local)*	*Lat*	*Lon*	M_w	*Met*	*Depth (km)*	*F.M.*	*Reference*	*Location*	*Source*
51	1930 07 23	23:00	41.050	15.370	6.7	LP	14	RL	JIM, CPTI	Irpinia	GG
56	1950 09 05	04:08	42.516	13.657	5.7	Pol	10-20	NF	GAS85	Gran Sasso	GG
59	1958 06 24	06:07	42.340	13.477	5.1	Pol	-	NF	GAS85	Aquilano	
78	1962 08 21	18:09	41.135	15.017	5.7	Pol	8-25	NF	GAS85, WE87	Irpinia	
60	1962 08 21	18:19	41.130	14.970	6.2	Pol	8-25	NF	GAS85, WE87	Irpinia	MS
79	1962 08 21	18:44	41.180	15.090	6.0	Pol	8-25	LL	GAS85	Irpinia	
80	1967 09 12	03:09	42.000	16.500	4.7	Pol	20-25	NF	GAS85	Southern Adriatic Sea	
62	1971 05 06	03:45	41.150	15.233	5.2	Pol	18-22	RL	GAS85, CPTI	Monteleone	
63	1971 11 29	18:49	40.500	15.800	4.8	Pol	5-20	RL	GAS85, VG04, CPTI	Marsico	
81	1973 08 08	14:36	40.720	15.410	4.8	Pol	5	LL	GAS85, VG04, CPTI	Picentini Mts.	
82	1973 10 30	01:14	41.700	13.870	4.7	Pol	5	RL	GAS85, VG04	Val Comino	
64	1975 06 19	10:11	41.650	15.730	5.0	Pol	18	RL	GAS85, CPTI	Gargano	
83	1978 09 24	08:07	40.797	16.109	4.5	Pol	20-28	NF	GAS85, VG04	Irsina	
68	1980 11 23	18:34	40.850	15.280	6.9	Pol, CMT	13	NF	GIA, VG04	Irpinia - Basilicata	GG
84	1980 11 25	18:28	40.650	15.390	5.4	CMT	15	NF	HAR	Irpinia	
85	1981 01 16	00:37	40.880	15.450	5.2	CMT	15	NF	HAR	Irpinia	
70	1984 05 07	17:49	41.670	14.057	5.9	CMT	13	NF	WE89, PA02	Abruzzo	GG
86	1984 05 11	10:41	41.708	13.880	5.5	CMT	11	NF	WE89, HAR	Abruzzo	
87	1986 01 18	09:32	41.595	14.225	4.0	Pol	8	LL	ALE90, CAST	Isernia	
71	1986 07 23	08:19	40.626	15.705	4.6	Pol	15	RL	ALE95, CPTI	Potentino	
88	1988 04 26	00:53	42.250	16.650	5.4	CMT	15-25	TF	HAR, LOUV, CAST	Central Adriatic Sea	
72	1990 05 05	07:21	40.640	15.860	5.8	CMT	22	RL	AZ93, EKS, CAST	Potenza	GG
73	1991 05 26	12:25	40.668	15.803	5.2	CMT	20	RL	EKS, CAST	Potenza	
89	1992 03 18	16:29	41.233	14.816	4.0	Pol	12	RL	FA0A, VG04	Beneventano	
74	1992 07 16	05:38	42.110	14.110	4.3	Pol	18-22	RL	FA0A, VG04, CAST	Guardiagrele	
75	1995 09 30	10:14	41.754	15.656	5.2	Pol	22-27	RL	FA0A, VG04, CAST	Gargano	
90	1996 04 03	13:04	40.657	15.438	4.9	Pol	8	NF	CO99, CAST	Irpinia	
91	1997 03 19	23:10	41.416	14.650	4.1	Pol	13-15	NF	MI99, CAST	Matese	
92	2001 07 02	10:04	42.000	15.450	4.5	CMT	10-20	NF	ETH, MED	Gargano	
93	2002 04 18	20:56	40.584	15.541	4.4	CMT	8	NF	MED, CAST	Irpinia - Basilicata	
76	2002 10 31	10:32	41.630	14.770	5.8	CMT	25	RL	PO03, CAST, VALL	Molise	GG
77	2002 11 01	15:09	41.680	14.990	5.8	CMT	21	RL	PO03, CAST, VALL	Molise	GG
94	2002 11 01	17:21	41.650	14.910	4.5	CMT	10-20	RL	MED	Molise	
95	2003 06 01	15:45	41.610	14.850	4.4	CMT	17	RL	MED	Molise	
96	2003 11 14	00:21	40.339	14.568	4.6	CMT	-	RL	ETH	S. Tyrrhenian Sea	
97	2003 12 30	05:31	41.680	14.830	4.5	CMT	15-20	RL	MED	Molise	
98	2004 09 03	04:12	40.701	15.684	4.4	CMT	20-30	RL	MED	Potentino	
99	2006 05 29	02:20	41.800	15.900	4.6	Pol, CMT	20-30	RL	MED	Gargano	

100	2006 10 04	17:34	42.010	15.680	4.3	CMT	30-40	RL	MED	Isole Tremiti

Table 1

Intensity data for the three main events of the 1456 sequence

Locality	Lon	Lat	I_new	#	Locality	Lon	Lat	I_new	#
Accadia	15.334	41.158	8.0	**1**	Cuma	14.056	40.849	5.5	**1**
Acerra	14.373	40.943	8.0	**1**	Dugenta	14.452	41.132	8.5	**1**
Acquaviva d'Isernia	14.149	41.672	10.0	**2**	Durazzano	14.446	41.063	9.0	**1**
Alberona	15.123	41.432	8.0	**1**	Ercolano	14.349	40.807	5.0	**1**
Alife	14.330	41.328	9.0	**1**	Ferrazzano	14.672	41.530	10.0	**2**
Alvito	13.742	41.689	8.0	**2**	Foggia	15.553	41.460	5.0	**2**
Amalfi	14.603	40.634	5.5	**1**	Fondi	13.427	41.358	8.0	**2**
Andria	16.296	41.226	5.0	**1**	Forlì del Sannio	14.179	41.695	9.0	**2**
Apice	14.931	41.118	11.0	**1**	Formia	13.617	41.261	7.0	**2**
Aquilonia Vecchia	15.494	40.996	9.0	**1**	Fornelli	14.140	41.607	9.0	**2**
Ariano Irpino	15.089	41.153	11.0	**1**	Fossalto	14.545	41.672	9.0	**2**
Arienzo	14.499	41.022	8.0	**1**	Fragneto l'Abate	14.785	41.259	8.5	**1**
Arpaia	14.547	41.035	8.0	**1**	Fragneto Monforte	14.761	41.246	9.0	**1**
Ascoli Satriano	15.561	41.205	8.0	**1**	Francolise	14.054	41.185	8.0	**1**
Atella	15.653	40.877	8.0	**1**	Frigento	15.099	41.011	10.0	**1**
Avellino	14.791	40.914	9.0	**1**	Frosolone	14.448	41.600	10.0	**2**
Aversa	14.207	40.974	8.0	**1**	Gaeta	13.568	41.218	7.0	**2**
Baia	14.071	40.817	5.5	**1**	Grottaminarda	15.057	41.069	9.5	**1**
Baranello	14.554	41.527	9.0	**2**	Guardia Sanframondi	14.596	41.255	9.0	**1**
Bari	16.846	41.106	6.5	**1**	Guardiaregia	14.542	41.435	9.0	**2**
Barletta	16.279	41.318	5.0	**1**	Isernia	14.231	41.594	11.0	**2**
Benevento	14.777	41.129	8.5	**1**	L'Aquila	13.396	42.356	5.0	**3**
Biccari	15.194	41.396	7.0	**1**	Lacedonia	15.424	41.049	9.0	**1**
Bitonto	16.691	41.108	5.5	**1**	Lanciano	14.390	42.230	5.5	**3**
Bojano	14.469	41.484	11.0	**2**	Lecce	18.169	40.351	5.5	**1**
Bonito	15.004	41.102	10.0	**1**	Limata	14.613	41.231	10.0	**1**
Bovino	15.342	41.251	8.0	**1**	Limosano	14.621	41.675	9.0	**2**
Brindisi	17.945	40.636	5.5	**1**	Lucera	15.335	41.508	8.0	**2**
Busso	14.559	41.556	9.0	**2**	Macchiagodena	14.405	41.558	10.0	**2**
Calvi Vecchia	14.137	41.203	7.0	**1**	Manfredonia	15.908	41.623	5.5	**2**
Campobasso	14.667	41.557	9.0	**2**	Marigliano	14.457	40.924	7.0	**1**
Campochiaro	14.505	41.449	9.0	**2**	Melfi	15.653	40.994	8.5	**1**
Canosa di Puglia	16.066	41.223	9.0	**1**	Mercato San Severino	14.759	40.785	7.5	**1**
Cantalupo nel Sannio	14.393	41.521	9.0	**2**	Minturno	13.746	41.263	7.5	**2**
Capua	14.214	41.106	7.5	**1**	Mirabella Eclano	14.996	41.042	10.0	**1**
Caramanico Terme	14.002	42.157	10.5	**3**	Miranda	14.247	41.641	9.0	**2**
Carinola	13.978	41.188	7.0	**1**	Mola di Bari	17.088	41.057	5.5	**1**
Carpinone	14.325	41.592	9.0	**2**	Monopoli	17.296	40.951	5.5	**1**
Casacalenda	14.848	41.740	9.0	**2**	Montecalvo Irpino	15.034	41.196	9.0	**1**
Casalciprano	14.528	41.579	10.0	**2**	Montecassino	13.814	41.490	6.0	**2**
Casalduni	14.695	41.260	10.0	**1**	Montecorvino	15.150	41.518	9.0	**2**
Cassino	13.830	41.488	7.0	**2**	Monteleone	14.820	41.249	10.0	**1**
Castel di Sangro	14.108	41.783	9.0	**2**	Monticchio	15.556	40.927	7.0	**1**
Castel San Vincenzo	14.063	41.655	9.0	**2**	Montoro Superiore	14.800	40.817	9.0	**1**
Castelcicala	14.555	40.917	9.0	**1**	Morcone	14.664	41.340	10.0	**1**
Castellammare di Stabia	14.486	40.700	8.0	**1**	Napoli	14.260	40.855	8.0	**1**
Castellino del Biferno	14.731	41.701	9.0	**2**	Navelli	13.729	42.236	8.5	**3**
Castellone al Volturno	14.067	41.657	9.0	**2**	Nola	14.529	40.926	7.0	**1**
Castelluccio Acquaborrana	14.710	41.828	9.0	**2**	Oratino	14.586	41.584	9.0	**2**
Castelluccio Valmaggiore	15.198	41.341	8.0	**1**	Paduli	14.880	41.164	11.0	**1**
Castelnuovo	13.628	42.295	8.5	**3**	Pago Veiano	14.871	41.247	9.0	**1**
Castelpetroso	14.346	41.559	9.0	**2**	Palma Campania	14.554	40.868	9.0	**1**
Castiglione a Casauria	13.900	42.235	9.0	**3**	Penne	13.928	42.457	5.0	**3**
Castropignano	14.561	41.618	9.0	**2**	Pesche	14.281	41.610	9.0	**2**
Cava de' Tirreni	14.706	40.700	5.5	**1**	Pesco Sannita	14.812	41.234	11.0	**1**
Cercemaggiore	14.722	41.460	10.0	**2**	Pescocostanzo	14.065	41.889	8.0	**2**
Cercepiccola	14.666	41.459	10.0	**2**	Pescolanciano	14.336	41.678	9.0	**2**
Cerreto Sannita	14.560	41.284	9.0	**1**	Pettoranello del Molise	14.277	41.573	9.0	**2**
Cerro al Volturno	14.102	41.656	9.0	**2**	Pietraroja	14.549	41.346	9.0	**1**
Chieti	14.168	42.351	5.0	**3**	Pietrelcina	14.848	41.197	8.0	**1**
Civitanova del Sannio	14.404	41.666	8.0	**2**	Pizzone	14.035	41.667	8.0	**2**
Civitella Licinio	14.527	41.309	10.5	**1**	Polignano a Mare	17.219	40.994	5.5	**1**
Colle d'Anchise	14.519	41.509	9.0	**2**	Pompei	14.501	40.749	5.0	**1**

Locality	Lon	Lat	I_new	#
Corsano	14.990	41.180	9.0	**1**
Covatta	14.606	41.631	9.0	**2**
Popoli	13.833	42.171	8.5	**3**
Pozzuoli	14.123	40.822	5.5	**1**
Pratola Peligna	13.875	42.098	9.0	**3**
Rapolla	15.675	40.975	8.0	**1**
Reino	14.824	41.291	9.0	**1**
Riccia	14.836	41.484	9.0	**2**
Rionero Sannitico	14.140	41.711	9.0	**2**
Ripalimosani	14.665	41.612	8.0	**2**
Rivisondoli	14.066	41.870	9.0	**2**
Rocca Pia	13.977	41.932	9.0	**3**
Roccacinquemiglia	14.121	41.811	9.0	**2**
Roccarainola	14.561	40.971	9.0	**1**
Roccaraso	14.079	41.847	9.0	**2**
Roccasicura	14.234	41.696	10.0	**2**
Roccaspromonte	14.560	41.599	9.0	**2**
Rocchetta a Volturno	14.088	41.623	9.0	**2**
Salerno	14.765	40.679	7.0	**1**
San Bartolomeo in Galdo	15.016	41.411	9.0	**1**
San Clemente a Casauria	13.929	42.234	9.0	**3**
San Donato Val di Comino	13.812	41.708	8.0	**2**
San Giorgio la Molara	14.919	41.270	10.0	**1**
San Giuliano del Sannio	14.639	41.456	10.0	**2**
San Lupo	14.635	41.260	11.0	**1**
San Marco dei Cavoti	14.878	41.308	10.0	**1**
San Massimo	14.411	41.493	9.0	**2**
San Pietro Avellana	14.182	41.789	9.0	**2**
San Polomatese	14.494	41.459	10.0	**2**
Sant'Agata de' Goti	14.504	41.088	8.5	**1**
Sant'Angelo in Grotte	14.372	41.562	10.0	**2**
Sant'Angelo Limosano	14.604	41.692	9.0	**2**
Santa Maria di Realvalle	14.547	40.764	9.0	**1**
Santa Maria in Galdo Mazzocca	14.886	41.373	9.0	**1**
Santo Stefano	14.610	41.612	10.0	**2**
Sarno	14.621	40.813	9.0	**1**
Sassinoro	14.663	41.374	9.0	**1**
Scapoli	14.057	41.615	9.0	**2**
Sepino	14.619	41.407	9.0	**1**
Sessa Aurunca	13.934	41.236	7.0	**1**
Sessano del Molise	14.332	41.636	9.0	**2**
Somma Vesuviana	14.437	40.872	8.5	**1**
Sora	13.613	41.718	7.0	**2**
Sorrento	14.378	40.624	5.0	**1**
Spina	14.119	41.698	9.0	**2**
Spinete	14.487	41.542	9.0	**2**
Sprondasino	14.457	41.729	9.0	**2**
Sulmona	13.928	42.047	8.0	**3**
Taranto	17.246	40.458	5.5	**1**
Teano	14.068	41.251	7.0	**1**
Termoli	14.993	42.000	5.5	**3**
Tocco Caudio	14.627	41.124	9.5	**1**
Tocco da Casauria	13.913	42.213	10.0	**3**
Torella del Sannio	14.520	41.639	9.0	**2**
Toro	14.766	41.570	9.0	**2**
Torre de' Passeri	13.933	42.244	9.0	**3**
Tramonti	14.641	40.694	8.0	**1**
Trani	16.418	41.277	5.5	**1**
Troia	15.309	41.361	8.0	**1**
Tufara	14.948	41.481	9.0	**2**
Vairano Patenora	14.132	41.333	8.0	**1**
Vasto	14.708	42.116	5.5	**3**
Venafro	14.044	41.485	8.5	**2**
Pontecorvo	13.667	41.456	9.0	**2**
Pontelandolfo	14.693	41.286	9.0	**1**
Venosa	15.818	40.961	8.0	**1**
Vieste	16.179	41.882	5.5	**2**
Vinchiaturo	14.587	41.493	10.0	**2**
Vittorito	13.817	42.125	9.0	**3**
Vitulano	14.646	41.174	9.0	**1**
Volturino	15.124	41.478	9.0	**2**
Zungoli	15.203	41.123	7.0	**1**

Table 2

Figure and Table Captions

Figure 1

Macroseismic maps of the 1456 earthquake prior to this work (original graphic layout slightly modified). *a)* original dataset by Magri and Molin (1983); *b)* study by Meletti et al. (1988); *c)* review made for the Catalog of Strong Italian Earthquakes (data from: Boschi et al., 2000). For ease of reading, intensity is plotted using Arabic numerals in all figures (e.g. 7.5) instead of using the standard Latin numerals (i.e. VII/VIII), which we use in the main text. In *c)*, we show isoseismals computed using the Multiquadric Radial Basis Function (algorithm from Carlson and Foley, 1992; see application in Fracassi et al., 2005).

Figure 2

Simplified geological map of central and southern Italy (from Butler et al., 2004, modified). The main tectonic units are (from west to east): the Mesozoic-Paleogene Apennines inner carbonate platform (hinterland), the Mesozoic-Neogene Lagonegro pelagic basin, and the Mesozoic-Paleogene Apulian carbonate platform (foreland). East of the outer Apennines front, the Bradano-Candela Foredeep hosts Plio-Quaternary terrigenous deposits. Jurassic-Oligocene Liguride units are present southwest of the studied area. Volcanic districts concentrate along the Tyrrhenian coast, except for the extinct Vulture complex, situated within the southern Apennines close to the external thrust front.

Figure 3

Historical and instrumental earthquakes (M > 4.0) of central and southern Italy (data in Table 1). Squares (proportional to magnitude) are events from Italy's current historical catalog (Gruppo di Lavoro CPTI, 2004); beachballs show focal mechanism of instrumental events. Notice the predominance of (a) dip-slip focal mechanisms on NW-SE trending planes in the core of the thrustbelt and (b) strike-slip mechanisms in the eastern sector of the Apennines and in the Apulian foreland (evidence of the E-W plane being the fault plane comes from events *72*, *73*, *76* and *77*). Also notice reverse faulting mechanisms northeast of the Gargano promontory. Focal mechanisms were generated using BeachBalls 1.0 (courtesy of R. Basili, INGV). Dark boxes indicate location of 1456 mainshocks in current catologs (Gruppo di Lavoro CPTI, 2004).

Figure 4

Cumulative spatial distribution of intensities caused by the 1456 sequence. Notice the very broad region where intensities > X were recorded, particularly in the Sannio area (east of Benevento), northeast of the Matese massif (between Isernia and Campobasso), and in the northwestern slope of the Maiella Mt. Also notice 1) the intermediate to low damage felt along the

Adriatic coast, and 2a) the group of high intensities (~ IX) between the Sannio, Irpinia and Capitanata regions, and 2b) in the Piana Campana. Figs. 5a, b and c provide close-ups on the areas of maximum damage.

Figure 5

Areas of maximum cumulative damage caused by the 1456 sequence. Location of areas *a*, *b*, and *c* in inset (lower right).

Figure 6

Time windows of 1456-1457 events based on (i) parameterized characteristics of writing style of the historical reports, and (ii) ratio of casualties/inhabitants inferred from coeval historical references (Guidoboni and Comastri, 2005). Dates in the cumulative legend are those imprinted on the manuscripts describing earthquake effects and thus do not directly reflect the date of the known mainshocks. Reported damage is dated (yyyy-mm-dd): *(a)*: 1456-12-06, -12-07, -12-08, -12-09, -12-11; *(b)*: 1456-12-12, -12-14; *(c)*: 1456-12-22; *(d)*: 1457-01; *(e)*: 1457-01-14; *(f)*: damage, not already described in previous coeval accounts, extracted from the 1457 report. Contours envelop areas for which peak intensities were reported (epicentral zones), except for coastal Apulia (eastern portion in *f*); datapoints with associated intensity values indicate localities which likely suffered shaking effects during more than one event. Scale in *a* through *e* is the same (shown in *a*).

Figure 7

Seismogenic areas based on the historical sequence of effects (bright patches; numbering is in progressive order of occurrence). For each event, we list moment magnitude (M_w) and corresponding seismic moment released (M_o). The *macroseismic sources* (black boxes) were computed from the intensity data using the Boxer ® code (see procedure in: Gasperini et al., 1999) for each sub-area, including source parameters (inset in lower left). Stars are centroid of the macroseismic source, i.e. the epicenter computed by Boxer, not that listed in the Italian historical catalog.

Figure 8

Proposed *seismogenic sources* for the three largest 1456 events, lettered in order of occurrence. Bar attached to the box is the surface projection of the fault plane; arrow showing the rake is always on the down-dip end of the fault plane. Large arrows show horizontal stress orientations after Montone et al. (2004). Note that the proposed faults (particularly the largest ones, i.e. ***A*** and ***B***) are constrained by the location of the published seismogenic sources (in orange) that caused the largest historical and instrumental earthquakes (years next to faults). NE-SW trending extensional faults coincide with the main axis of the southern Apennines, whereas E-W trending right-lateral strike-slip faulting occurs towards the Apulian foreland (sources from: DISS Working Group, 2006, and references therein; source parameters can be downloaded from: http://www.ingv.it/DISS/). Oblique slip on ~E-W oriented planes for the proposed 1456 sources (in red) would mark the transition from a purely extensional domain in the mountain belt (i.e., represented by the 1980 Irpinia earthquake) to a strike-

slip stress field in the foreland (i.e., represented by the 2002 Molise earthquakes). We consider the 1930 Irpinia event as a template for such transition. The ~E-W structures known in the subsurface are shown in green (Sella et al., 1988; Sawyer, 2001). The parameters of the seismogenic sources, based on empirical (Wells and Coppersmith, 1994) and analytical (Kanamori and Anderson, 1975) relationships, are summarized in lower left inset. Upper right inset describes geometrical parameters (determined using FaultStudio 1.2; courtesy of R. Basili, INGV).

Table 1

Earthquakes with M > 4 that occurred in the study area (see Fig. 3), historical (including recent ones for which macroseismic information is available) and instrumental (if a focal mechanism was available). ID is the identifier on Fig. 3; M_w is moment magnitude; Data n. is the number of validated localities where an intensity value exists in the macroseismic catalogs; Met is method (LP = long-period, Pol = polarities, CMT = centroid moment tensor) used to (re-)compute focal mechanisms (see references); F.M. indicates the focal mechanism (NF = normal fault; TF = thrust fault: RL = right-lateral strike-slip; LL = left-lateral strike-slip). When macroseismic data is available for an instrumental earthquake too, the latter is marked in **bold** and bears the same number of the historical listing. Source indicates presence and type of a published seismogenic fault in the literature (GG = determined via geological/ geomorphological/ geophysical data; MS = computed with macroseismic information only; data from: Valensise and Pantosti, 2001b; DISS Working Group, 2006, and references therein). Compared to the original datasets, for selected earthquakes we reduced the number of datapoints according to data reliability and/or relevance; also, in some cases we corrected the locality name according to the appropriate area.

Data references: BO00: Boschi et al. (2000) - CPTI: Gruppo di Lavoro CPTI (2004) - DOM: Monachesi and Stucchi (1997) - SGA: Guidoboni and Comastri (2005) - CA05: Castelli et al. (2005) - ISOS: INGV Isoseismal Atlas - INGV: INGV Macroseismic Atlas - RIG: Riguzzi (1999) - TERT: Tertulliani et al. (1992) - VALL: Vallée and Di Luccio (2005) - GA04: Galli and Molin (2004) - JIM: Jiménez (1991) - GAS85: Gasparini et al. (1985) - WE87: Westaway (1987) - VG04: Vannucci and Gasperini (2004) - GIA: Giardini (1993) - HAR: Harvard CMT (2005) - WE89: Westaway et al. (1989) - PA02: Pace et al. (2002) - ALE90: Alessio et al. (1990) - CAST: Castello et al. (2006) - ALE95: Alessio et al. (1995) - LOUV: Louvari and Kiratzi (2000) - AZ93: Azzara et al. (1993) - EKS: Ekström (1994) - FA0A: Frepoli and Amato (2000) - CO99: Cocco et al. (1999) - MI99: Milano et al. (1999) - MED: MEDNET (2006) - PO03: Pondrelli et al. (2003) - ETH: Schweizerischer Erdbebendienst (2005).

Table 2

Alphabetic record of localities and revised intensity values for the three 1456 main events. **I_new** lists the new intensities presented in this study; **#** indicates number of the *macroseismic source* with which the intensity point was associated (Fig. 6).

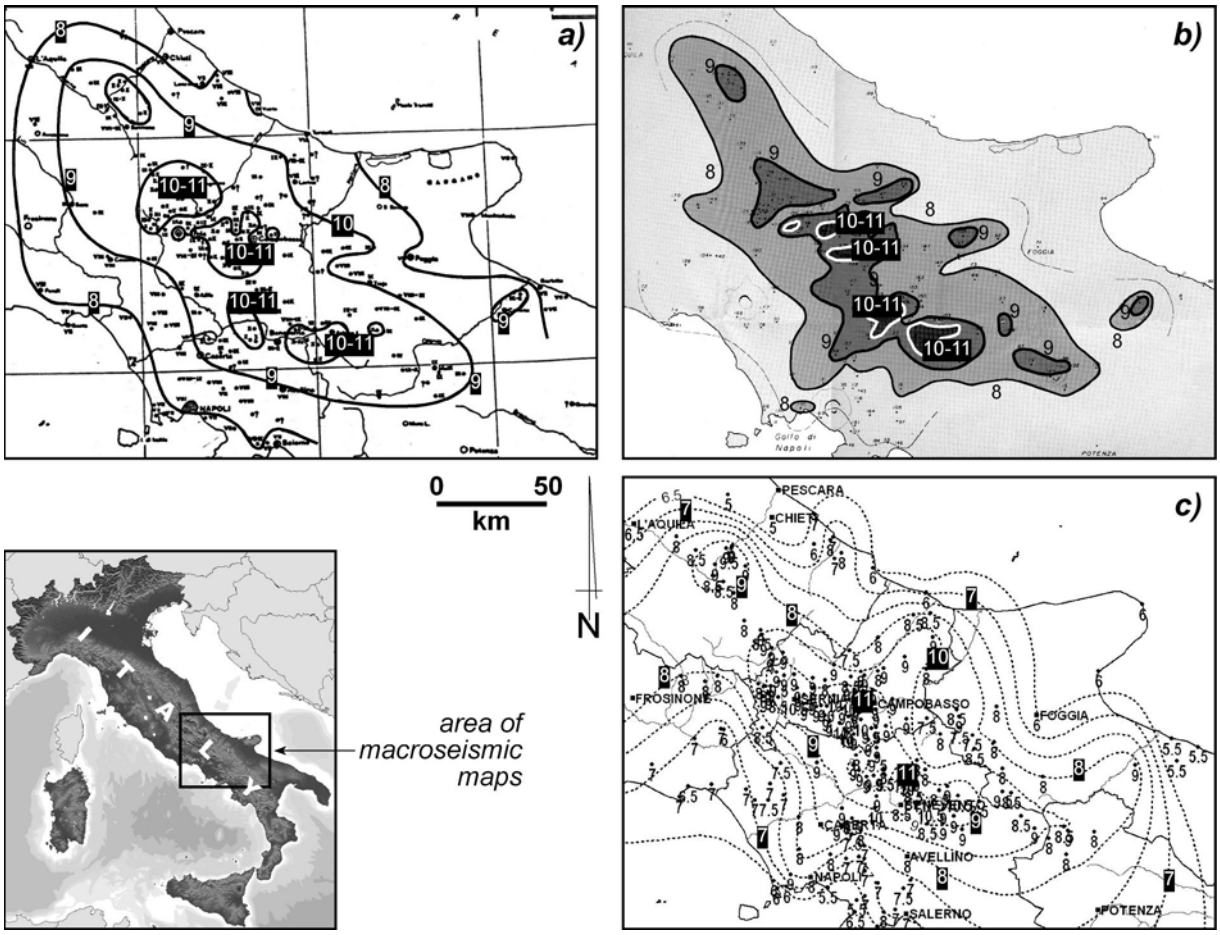
a)
b)
c)
0
50
km
N
I T A L Y
area of
macroseismic
maps
PESCARA
CHIETI
L'AQUILA
FROSINONE
CAMPOBASSO
FOGGIA
AVELLINO
NAPOLI
SALERNO
POTENZA

Fig. 1

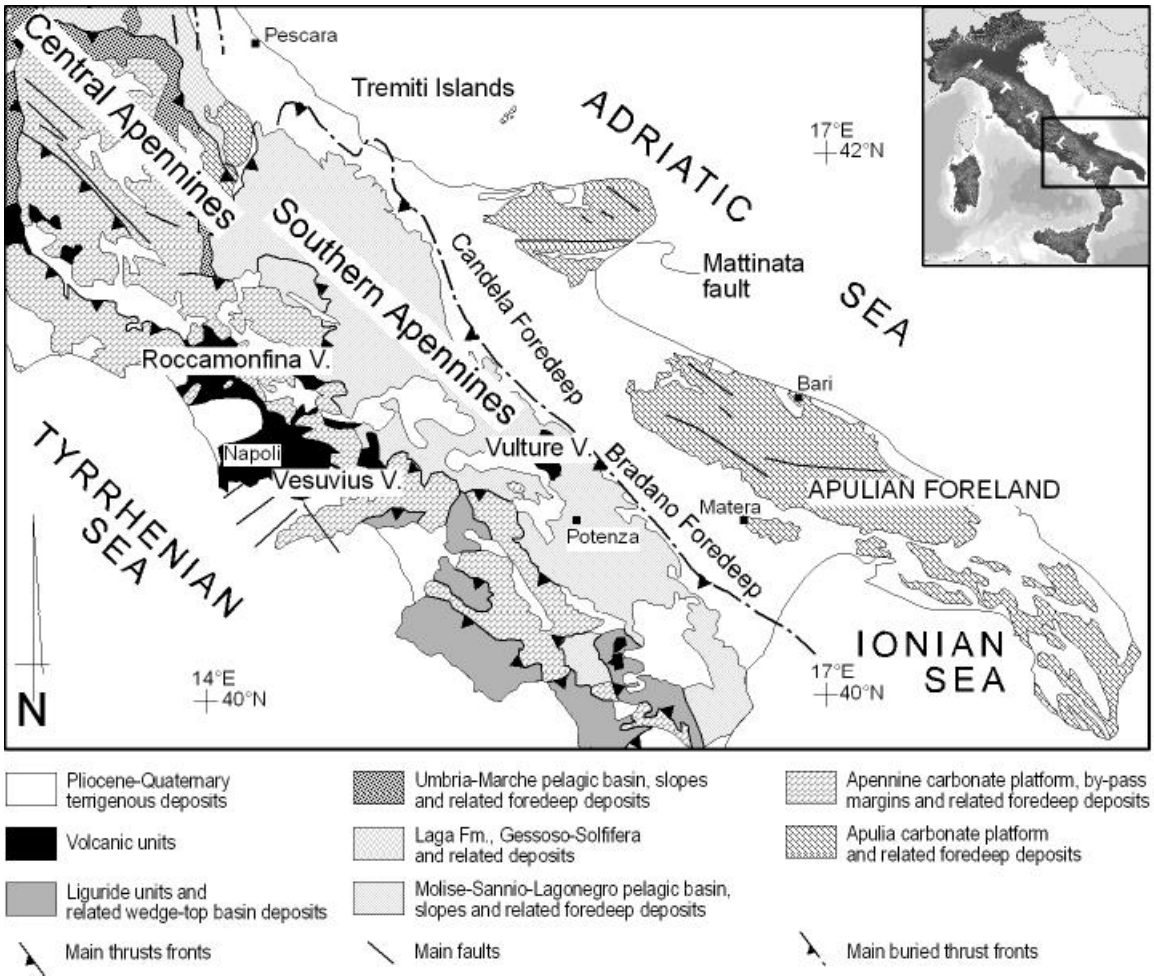
Pescara
Tremiti Islands
Central Apennines
Southern Apennines
ADRIATIC SEA
17°E
42°N
Candela Foredeep
Mattinata fault
Roccamonfina V.
Bari
Napoli
Vesuvius V.
Vulture V.
Bradano Foredeep
APULIAN FORELAND
Matera
Potenza
TYRRHENIAN SEA
IONIAN SEA
14°E
40°N
17°E
40°N
N
Pliocene-Quaternary terrigenous deposits
Volcanic units
Liguride units and related wedge-top basin deposits
Umbria-Marche pelagic basin, slopes and related foredeep deposits
Laga Fm., Gessoso-Solfifera and related deposits
Molise-Sannio-Lagonegro pelagic basin, slopes and related foredeep deposits
Apennine carbonate platform, by-pass margins and related foredeep deposits
Apulia carbonate platform and related foredeep deposits
Main thrusts fronts
Main faults
Main buried thrust fronts

Fig. 2

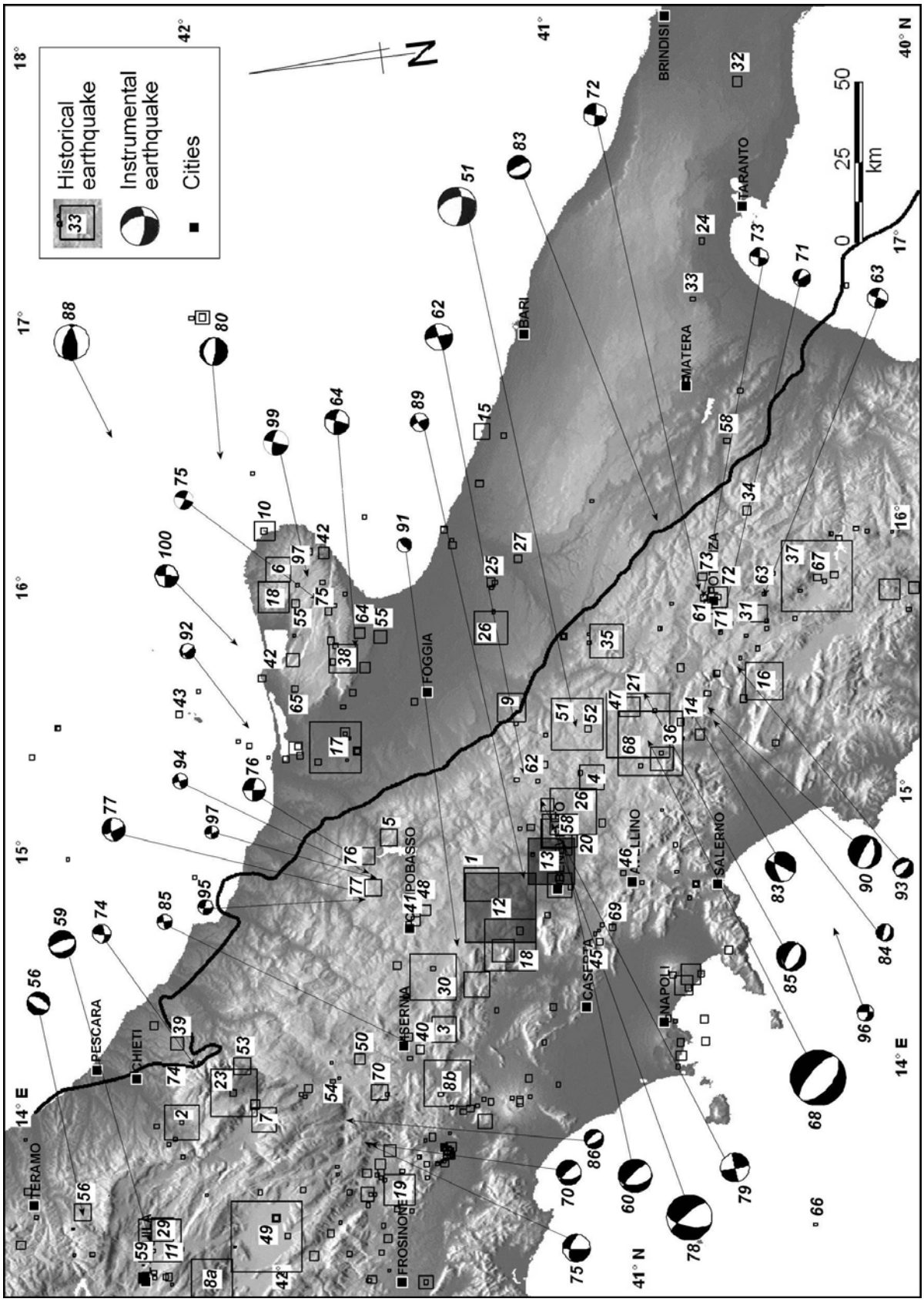
Historical earthquake
Instrumental earthquake
Cities
N
0
25
50
km
TERAMO
PESCARA
CHIETI
FROSINONE
ISERNIA
POBASSO
FOGGIA
BARI
BRINDISI
TARANTO
MATERA
SALERNO
NAPOLI
CASERTA
14° E
15°
16°
17°
18°
41° N
40° N

Fig. 3

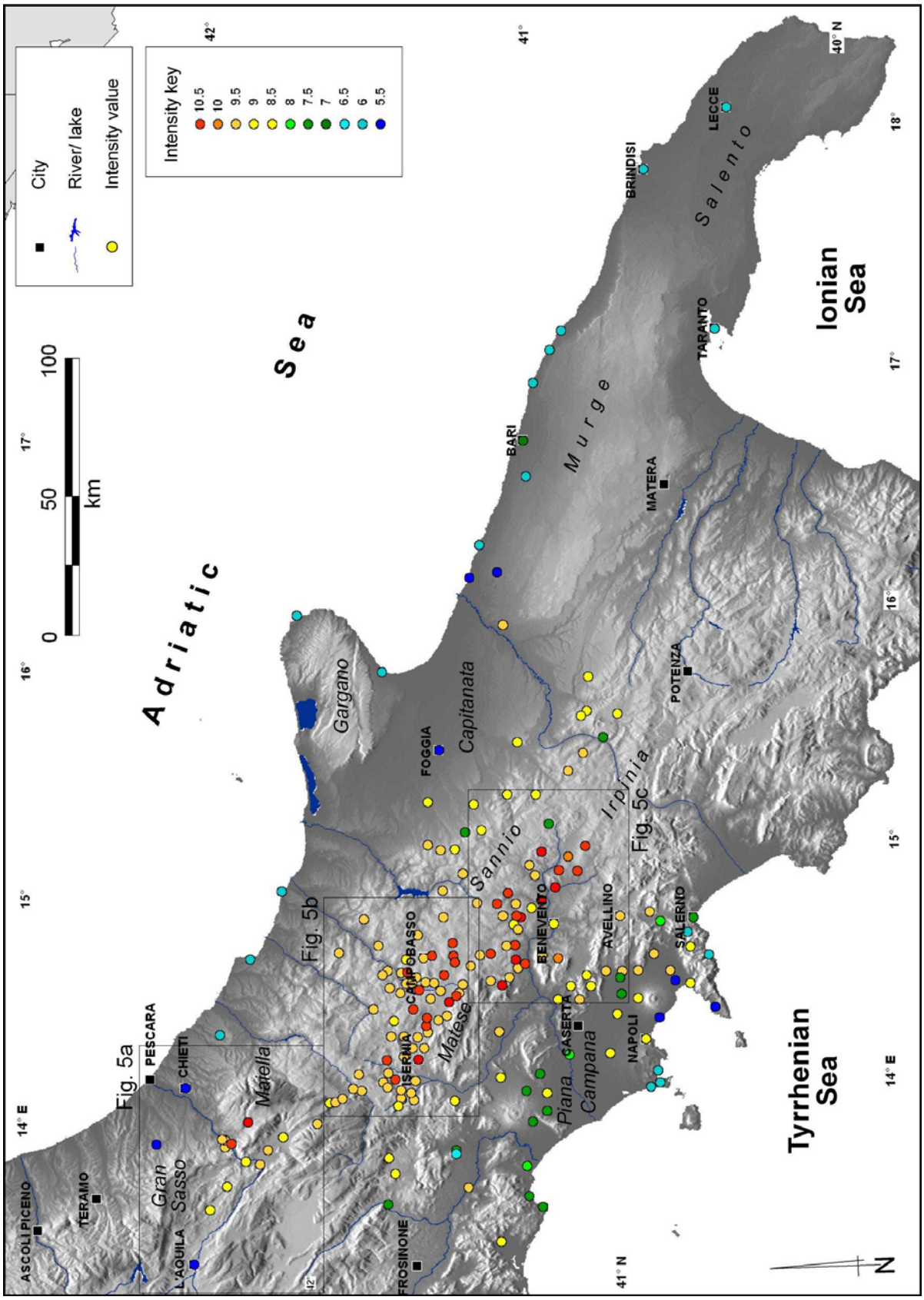
City
River/ lake
Intensity value
Intensity key
10.5
10
9.5
9
8.5
8
7.5
7
6.5
6
5.5
0
50
100
km
Adriatic Sea
Ionian Sea
Tyrrhenian Sea
Gargano
Capitanata
Murge
Salento
Sannio
Irpinia
Matese
Piana Campana
Gran Sasso
Marella
Fig. 5a
Fig. 5b
Fig. 5c
ASCOLI PICENO
TERAMO
PESCARA
CHIETI
L'AQUILA
FROSINONE
CAMPOBASSO
ISERNIA
FOGGIA
BARI
BRINDISI
LECCE
TARANTO
MATERA
POTENZA
BENEVENTO
AVELLINO
SALERNO
CASERTA
Nnapoli
14° E
15°
16°
17°
18°
42°
41°
41° N
40° N
N

Fig. 4

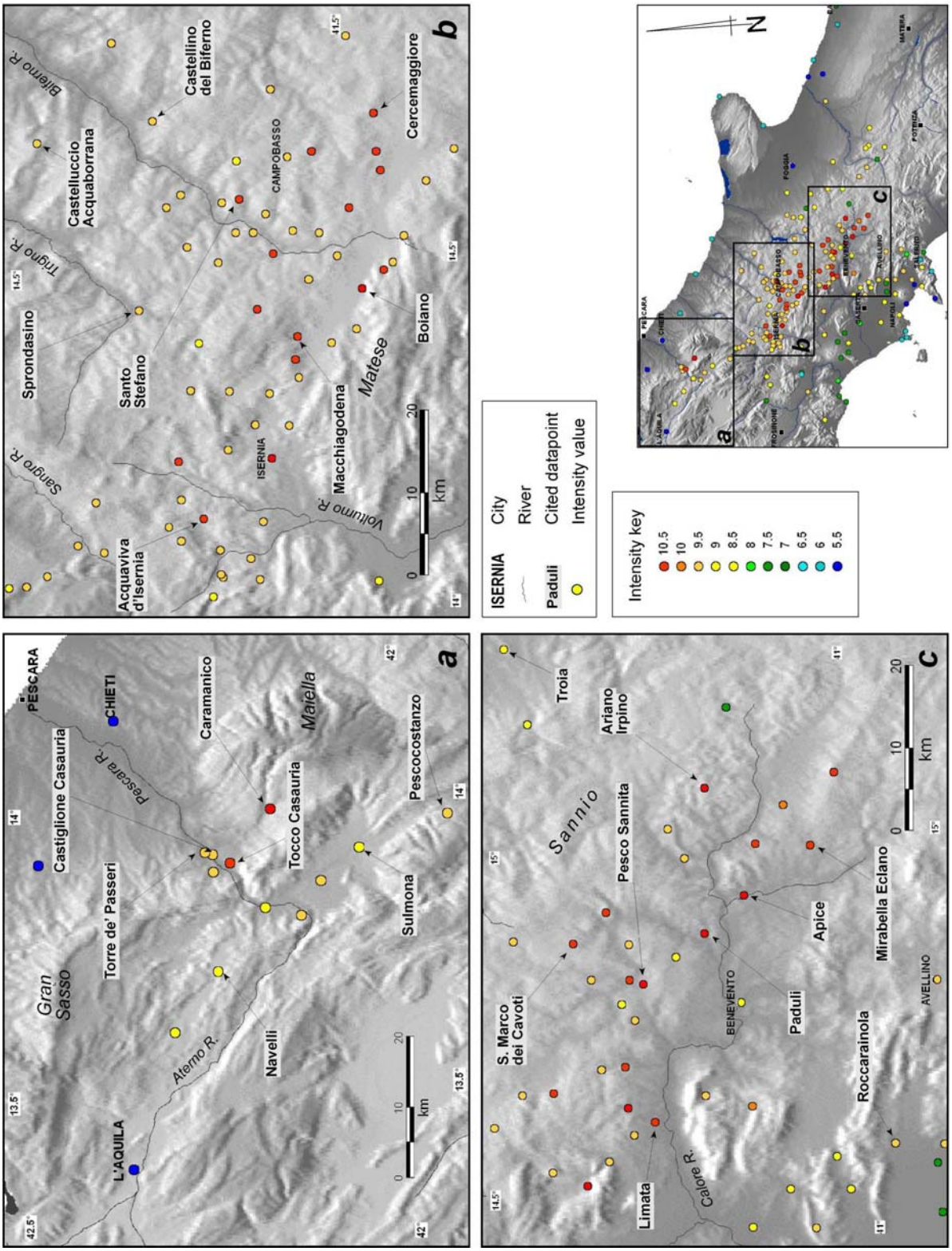
a
PESCARA
CHIETI
Castiglione Casauria
Pescara R.
Caramanico
Maiella
Gran Sasso
Torre de' Passeri
Tocco Casauria
Pescocostanzo
Sulmona
Aterno R.
Navelli
L'AQUILA
b
Biferno R.
Castelluccio Acquaborrana
Castellino del Biferno
Trigno R.
CAMPOBASSO
Cercemaggiore
Sprondasino
Santo Stefano
Matese
Boiano
Sangro R.
ISERNIA
Macchiagodena
Volturno R.
Acquaviva d'Isernia
c
Troia
Ariano Irpino
Sannio
Pesco Sannita
S. Marco dei Cavoti
BENEVENTO
Apice
Mirabella Eclano
Paduli
Roccarainola
AVELLINO
Limata
Calore R.
ISERNIA City
River
Paduli Cited datapoint
Intensity value
Intensity key
10.5
10
9.5
9
8.5
8
7.5
7
6.5
6
5.5
km
N

Fig. 5

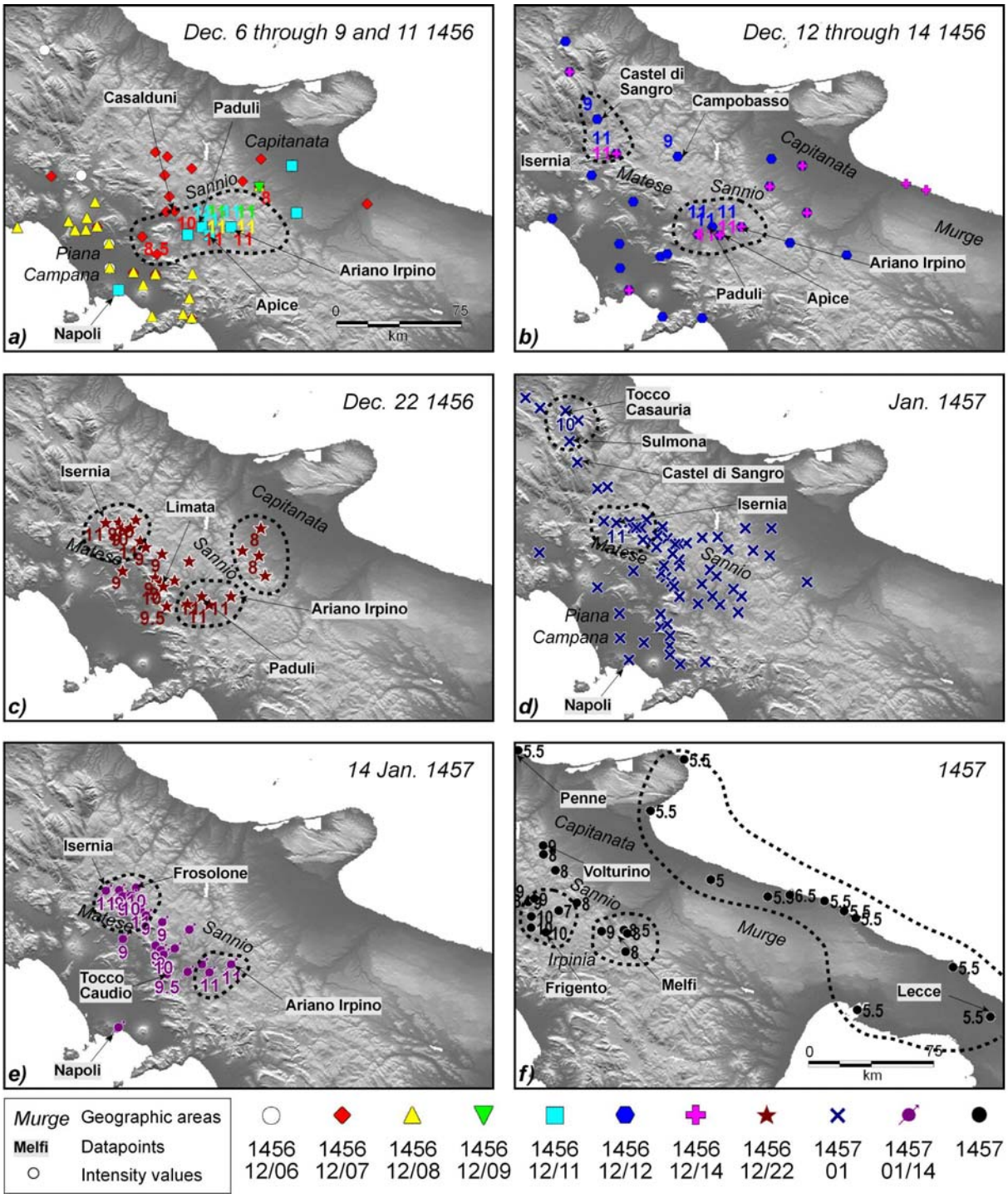
Dec. 6 through 9 and 11 1456
Casalduni
Paduli
Capitanata
Sannio
Piana
Campana
Ariano Irpino
Apice
Napoli
0
75
km
a)
Dec. 12 through 14 1456
Castel di Sangro
Campobasso
Isernia
Matese
Sannio
Capitanata
Murge
Ariano Irpino
Paduli
Apice
b)
Dec. 22 1456
Isernia
Limata
Capitanata
Matese
Sannio
Ariano Irpino
Paduli
c)
Jan. 1457
Tocco Casauria
Sulmona
Castel di Sangro
Isernia
Matese
Sannio
Piana
Campana
Napoli
d)
14 Jan. 1457
Isernia
Frosolone
Matese
Sannio
Tocco Caudio
Ariano Irpino
Napoli
e)
1457
Penne
Capitanata
Volturino
Sannio
Murge
Irpinia
Frigento
Melfi
Lecce
0
75
km
f)
Murge Geographic areas
Melfi Datapoints
Intensity values
1456 12/06
1456 12/07
1456 12/08
1456 12/09
1456 12/11
1456 12/12
1456 12/14
1456 12/22
1457 01
1457 01/14
1457

Fig. 6

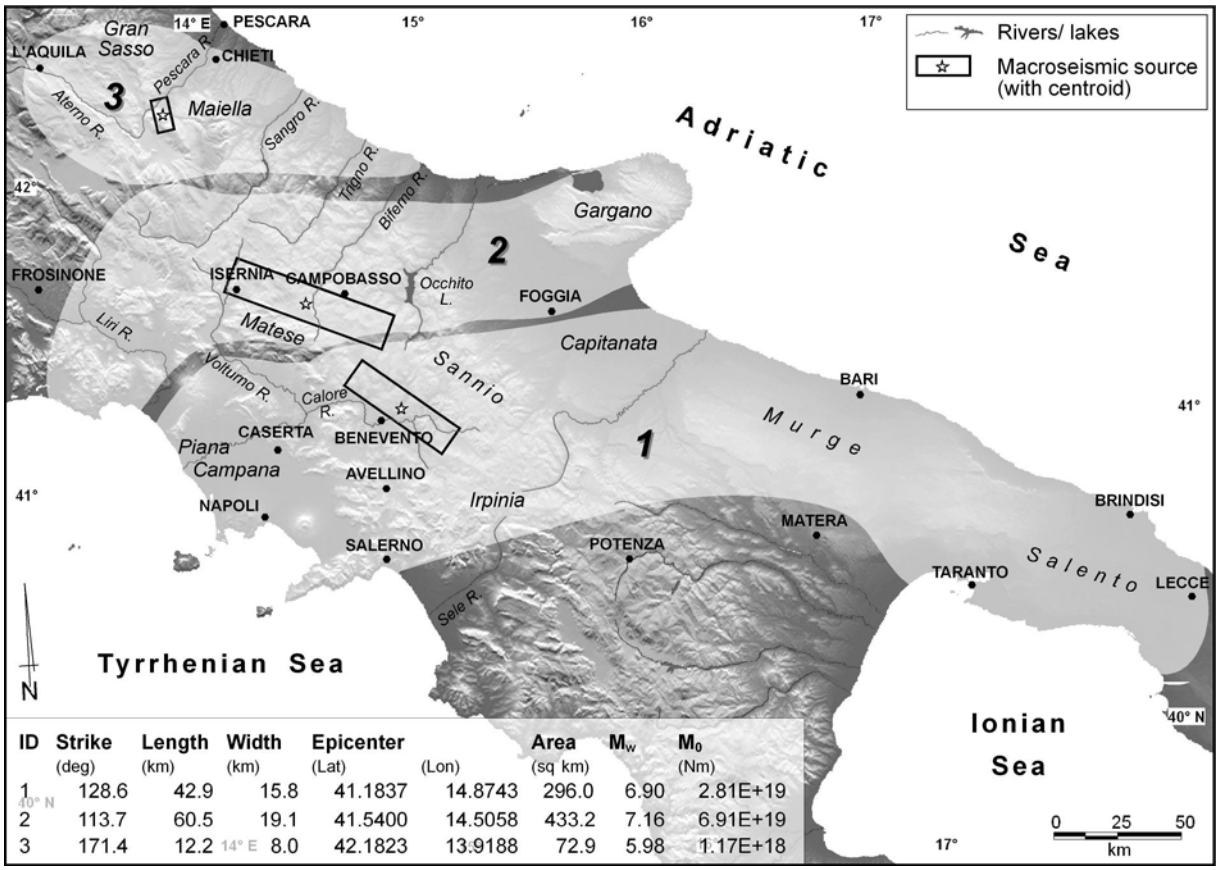

ID	Strike (deg)	Length (km)	Width (km)	Epicenter (Lat)	(Lon)	Area (sq km)	M_w	M_0 (Nm)
1	128.6	42.9	15.8	41.1837	14.8743	296.0	6.90	2.81E+19
2	113.7	60.5	19.1	41.5400	14.5058	433.2	7.16	6.91E+19
3	171.4	12.2	8.0	42.1823	13.9188	72.9	5.98	1.17E+18

Fig. 7

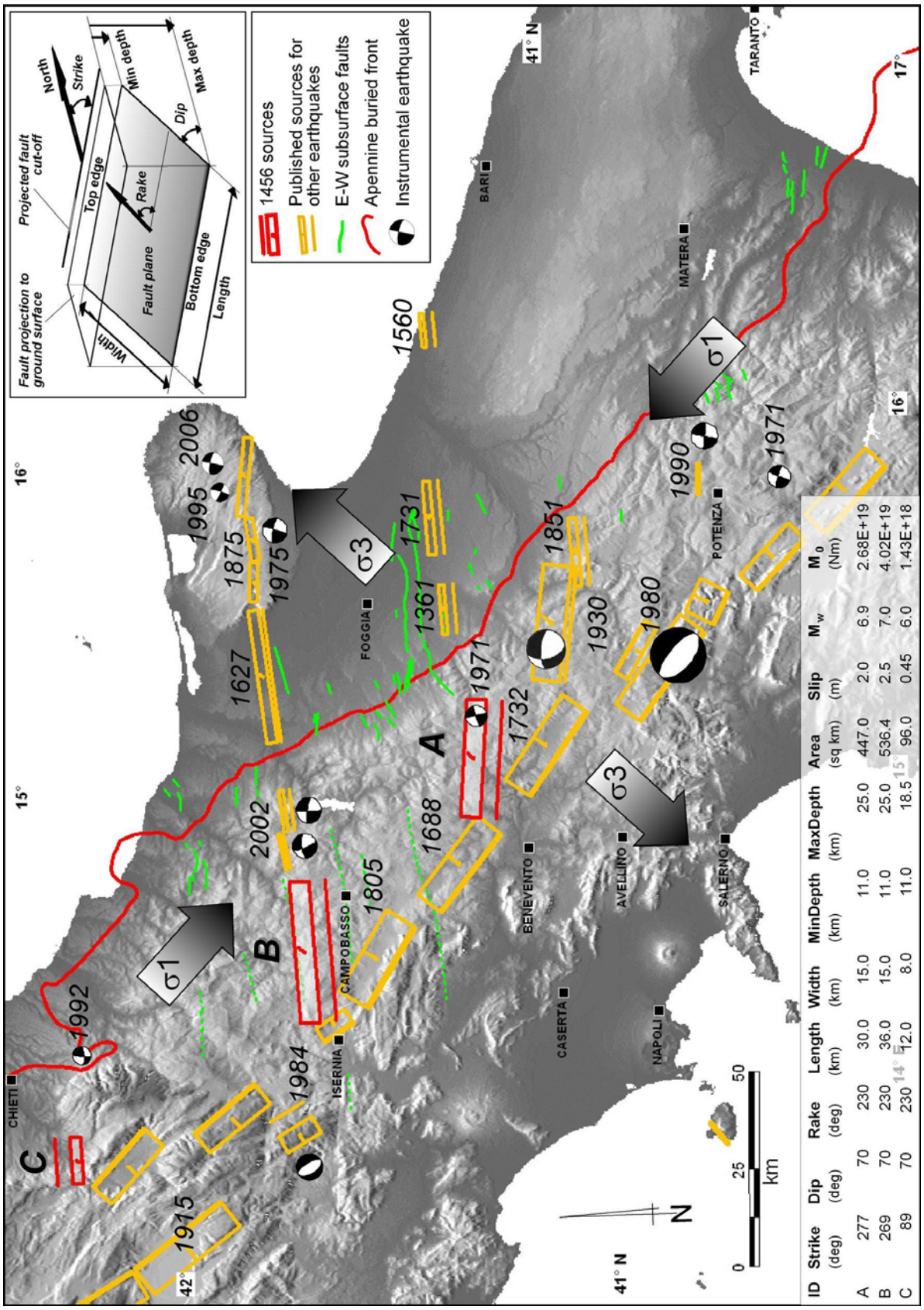

ID	Strike (deg)	Dip (deg)	Rake (deg)	Length (km)	Width (km)	MinDepth (km)	MaxDepth (km)	Area (sq km)	Slip (m)	M_w	M_o (Nm)
A	277	70	230	30.0	15.0	11.0	25.0	447.0	2.0	6.9	2.68E+19
B	269	70	230	36.0	15.0	11.0	25.0	536.4	2.5	7.0	4.02E+19
C	89	70	230	12.0	8.0	11.0	18.5	96.0	0.45	6.0	1.43E+18

Fig. 8